Effective *in vivo* RNA base editing *via* engineered cytidine deaminase APOBECs fused with PUF proteins

Wenjian Han [1, #, *], Bo Yuan [2, #], Xiaojuan Fan [3], Weike Li [4], Yiting Yuan [1], Yuefang Zhang[1], Shu Wang [1], Shifang Shan [4], Markus Hafner [3], Zefeng Wang [5, 6, *] & Zilong Qiu [1, 4, *]

[1] Department of Neurology, Songjiang Research Institute, Songjiang Hospital & MOE-Shanghai Key Laboratory for Children's Environmental Health, Shanghai Jiao Tong University School of Medicine, Shanghai, China

[2] Institute of Medical Genetics and Genomics, Fudan University, Shanghai, China

[3] RNA Molecular Biology Laboratory, National Institute of Arthritis and Musculoskeletal and Skin Disease, Bethesda, MD, USA.

[4] Institute of Neuroscience, Center for Excellence in Brain Science and Intelligence Technology, Chinese Academy of Sciences, Shanghai, China

[5] Shanghai Institute of Nutrition and Health, Chinese Academy of Sciences, Shanghai, China

[6] Southern University of Science and Technology, Shenzhen, Guangdong, China

[#] These authors contributed equally to this work.

*Co-corresponding authors: hanwenjian@shsmu.edu.cn (W.H.), wangzf@sustech.edu.cn (Z.W.), qiuzilong@shsmu.edu.cn (Z.Q.)

Summary

Base editing stands at the forefront of genetic engineering, heralding precise genetic modifications with broad implications. While CRISPR-based DNA and RNA base editing systems capitalize on sgRNA-guided specificity and diverse deaminase functionalities, the pursuit of efficient C-to-U RNA editing has been hampered by the inherent constraints of cytidine deaminases. Here, we report an RNA base editing platform by refining cytidine deaminases, termed professional APOBECs (ProAPOBECs), through systematic enhancements and AI-driven protein engineering. ProAPOBECs demonstrate unprecedented catalytic versatility, particularly fused with RNA-recognizing Pumilio and FBF (PUF) proteins. We demonstrated that *in vivo* RNA base editing of *Pcsk9* using ProAPOBECs effectively lowers cholesterol levels in mice. Additionally, AAV-mediated RNA base editing with ProAPOBECs in the brain of an autism mouse model not only corrected point mutations in *Mef2c* mRNAs but also significantly alleviated disease-associated phenotypes. This work introduces a pioneering collection of RNA base editing instruments, emphasizing their therapeutic potential in combatting genetic disorders.

Introduction

CRISPR-based base editing offers a potent method for editing genetic material by directly modifying single base pair in DNA or RNA. This approach, involving C-to-U (cytidine-to-uridine) and A-to-I (adenosine-to-inosine) transitions mediated by deaminases, avoids the strand breaks typically induced by the CRISPR/Cas system [1,2]. Initially developed for DNA modification, CRISPR/Cas-based targeting has become an effective tool in genetic research and holds potential for therapeutic applications, such as correcting disease-associated mutations in animal models [3-9].

Unlike the permanent modifications made by DNA base editing [10-12], RNA base editing offers a reversible method for *in vivo* base alternations, providing a relatively safer avenue for therapeutic strategies [13-17]. The A-to-I transition in RNA, mediated by Adenosine Deaminases Acting on RNA (ADAR), has been effectively demonstrated *in vivo* [18-20]. Two evolved ADAR2-based editing systems, RESCUE-S and xCBE, have been developed to achieve both A-to-I and C-to-U RNA editing [21,22]. However, RESCUE-S is strongly biased against editing G<u>C</u> and C<u>C</u> motifs, limiting its versatility [23]. To address this limitation, Stafforst's group introduced the SNAP-CDAR-S system, a SNAP-tag-based tool designed to edit C<u>C</u> motifs in specific RNA targets [24]. While promising, evolved ADAR2-mediated base editing systems, including SNAP-CDAR-S, exhibit simultaneous C-to-U and A-to-I off-target editing, imposing constraints on their broader application [21-24]. Engineering Apolipoprotein B mRNA editing enzyme catalytic polypeptide (APOBEC) family proteins offers a potential solution. These

proteins are specifically tailored for precise C-to-U base editing, effectively eliminating the A-to-I off-target effects and reducing undesired side effects. This approach represents a significant advancement in RNA base editing technology.

More recently, an RNA base editing system called CURE has been developed utilizing the dCasRx protein and a native APOBEC3A, to achieve limited yet specific UC transitions [23]. However, the specific Cas13-based C-to-U transition, has not achieved for efficiently correcting disease-causing mutations in mouse models [23,25]. One potential reason is the strong preference of APOBEC for single-stranded RNA, conflicting with the double-stranded structures formed by target mRNA and small guide RNA used in the CRISPR/Cas system [26].

To address existing limitations, the gRNA-free system, REWIRE (RNA editing with individual RNA-binding enzyme), was developed by exploiting the programmable RNA targeting capabilities of PUF proteins [27]. PUF proteins feature 8- or 10- repeat motifs, each of which can be programmed to specifically bind any RNA base *via* interaction with the Watson–Crick edge [28-32]. Various groups have developed PUF-based systems incorporating different functional domains to manipulate RNA splicing [33], translation [34], degradation [35] and methylation [36]. Given the versatility of PUF domain in recognizing nearly any short 8- or 10- nucleotide RNA sequences, its combination with ADAR or APOBEC enzymes allows REWIRE to perform precise and efficient A-to-I or C-to-U editing on specific nucleosides of RNA targets in cultured cells [27].

Notably, the use of mammalian-derived proteins in the REWIRE minimizes the potential immune responses often triggered by bacterial Cas enzymes in therapeutic base editing scenarios [37].

Current C-to-U RNA base editing systems rely on the enzymatic activity of APOBEC to hydrolytically deaminate cytidine [13,27]. Natural APOBECs, however, often exhibit deamination activity in a sequence context-dependent manner, primarily with single-strand DNA or RNA [38]. For instance, Human APOBEC3A preferentially edits cytidine within UC motifs in mRNA [23,27]. These context preferences limited further application of RNA base editors.

APOBEC enzymes, recognized for their critical role in inducing mutations within the genomes of retroviruses during infection, constitute a significant group of antiviral genes. Current NCBI database has documented over 8,231 eukaryotic genes homologous to the AID/APOBEC family, highlighting their extensive presence and diversity in eukaryotic organisms [39]. These AID/APOBEC proteins share a common domain configuration, with a highly conserved catalytic domain centered between the variable N-terminal (NTD) and C-terminal domain (CTD) [39-41], which may enable a rational design of novel cytidine deaminases using artificial intelligence-assisted protein engineering.

In this study, we use AlphaFold2-mediated structural engineering to develop

Professional APOBECs (ProAPOBECs) with greatly expanded C-to-U editing capability. When integrated within the REWIRE system, ProAPOBECs demonstrate improved specificity and efficiency in multiple sequence contexts, including GC, CC, AC, and UC.

Importantly, we achieved effective *in vivo* C-to-U RNA editing in the liver and brain of mice using the CU-REWIRE5s with ProAPOBECs delivered *via* adeno-associated virus (AAV). This *in vivo* RNA editing mediated by CU-REWIRE successfully reducing cholesterol levels in mice by targeting Pcsk9 mRNA and alleviated autistic-like behaviors by correcting a point mutation in Mef2c mRNA in an autism spectrum disorder (ASD) mouse model [8]. In conclusion, this study demonstrated that the AI-assisted protein engineering can be applied to refine the activity of RNA base editors, enabling the correction of autistic-like phenotype in mouse model and paving the way for the practical applications of RNA base editing in the realm of gene therapy.

Results

Enhanced Stability and Efficacy of CU-REWIRE *via* Structural Optimization of PUF Domain

Our initial efforts focused on improving CU-REWIRE3.0, which combined a 10-repeat PUF domain (PUF10) with the cytidine deaminase enzyme APOBEC3A. Structural analysis revealed high similarity between the fourth repeat (R4) of PUF10 in CU-REWIRE3.0 and the fifth repeat (R5) of the native Pumilio 2 protein. Importantly, R4

124 lacked the Leucine-Proline (LP) peptide present in R5, a potentially crucial element for
125 structural flexibility as suggested by the previous research [42]. This insight led us to
126 engineer an enhanced PUF10 (ePUF10) with the LP peptide integrated into R4,
127 resulting in the development of CU-REWIRE4.0 (Fig. 1a and Supplementary Fig. 1a).
128
129 Comparative analysis showed that CU-REWIRE4.0 exhibited higher expression
130 levels than its predecessor, suggesting improved stability due to the LP insertion (Fig.
131 1b). We then assessed the editing efficacy of CU-REWIRE4.0 by targeting the C-to-U
132 transition on the C_{459} site in the Enhanced Green Fluorescent Protein (EGFP) mRNA.
133 As judged by mRNA sequencing (mRNA-seq), the CU-REWIRE4.0 achieved a
134 substantial increase in editing efficiency, with an 82.3% success rate compared to 69.7%
135 for CU-REWIRE3.0 (Supplementary Fig. 1b).
136
137 To evaluate off-target effects, we conducted RNA-seq analysis with 50X
138 transcriptome coverage (See Methods). Four independent sample sets (APOBEC3A,
139 ePUF10, CU-REWIRE3.0, and CU-REWIRE4.0) were analyzed with mRNA-seq,
140 revealing 224 potential off-target events for CU-REWIRE3.0 and 731 for CU-
141 REWIRE4.0 (Supplementary Fig. 1c-e). Notably, none of the off-target sites were
142 within 20-nt downstream of ePUF10-binding sequences (Supplementary Fig. 1e),
143 suggesting a high precision of ePUF10 in recognizing target and a significantly lower
144 off-target rate compared to the earlier CU-REWIREs [27]. However, off-target events
145 were largely attributed to the basal activity of APOBECs, highlighting the need for

146 further optimization.

147

148 While showing promise in editing efficiency, the original CU-REWIRE3.0 was
149 restricted to C-to-U editing activity within the UC context [27]. Similar to its predecessors,
150 we found that the CU-REWIRE4.0 maintained the preference for editing cytidines
151 within the UC consensus motif (Supplementary Fig. 1f). Its precision was further
152 improved in that the C-to-U conversions predominantly occurred at the second position
153 downstream of the ePUF10 binding site (Supplementary Fig. 1g). We also applied CU-
154 REWIRE4.0 to specifically targeting the C_{832} site on the report mRNA of the mouse
155 *Pcsk9* gene. Our results revealed a marked improvement in C-to-U editing efficiency at
156 C_{832} with CU-REWIRE4.0 compared to CU-REWIRE3.0 (Supplementary Fig. 1h).
157 This underscores the enhanced specificity and efficiency of CU-REWIRE4.0.

158

159 **Structure-Based Optimization of APOBEC3A Minimizes Off-Target Effects**

160 APOBEC3A proteins tend to form dimers that stabilize their interaction with single-
161 stranded DNA or RNA [38]. While this interaction is key in inducing mutations in viral
162 genomes, it also contributes to bystander editing and off-target effects in non-target
163 genomic regions during base editing. Therefore, our next objective was to reduce
164 APOBEC3A dimerization.

165

166 By investigating the crystalline structure of APOBEC3A and building upon previous

research, we identified two amino acid sites (H11, C171) critical for dimerization [38]. The mutation of these sites could reduce the dimer formation and the association with nucleic acids of APOBEC3A (Fig. 1c). Additionally, two amino acids (K30, H56) were found to be involved in substrate RNA recognition by APOBEC3A [38]. Thus we speculate that mutations at these sites may diminish RNA recognition and, consequently, reduce off-target effects (Fig. 1d).

To test this possibility, we introduced various point mutations into human APOBEC3A (Fig. 1e). We then fused these mutated APOBEC3A versions with the ePUF10 domain, creating multiple CU-REWIRE4 variants that target C_{459} of EGFP mRNA expressed in HEK293T cells (Fig. 1f). After co-transfecting these constructs with the EGFP expressing plasmid, we evaluated the C-to-U editing efficiency at the C_{459} site of EGFP mRNA by these CU-REWIRE4 variants (Fig. 1g).

One variant, CU-REWIRE 4.1, with a C171A substitution in the C-terminal domain (CTD) of APOBEC3A, showed high editing efficiency while significantly reducing off-target effects (Fig. 1g, h). Interestingly, the CU-REWIRE 4.2, 4.4, and 4.5, each containing point mutations in the NTD, showed moderate editing efficiency but substantially minimized off-target events (Fig. 1g, h). These findings indicate that strategically designed point mutations in the NTD and CTD of APOBEC3A can significantly decrease off-target effects while maintaining sufficient editing efficiency

188 (Fig. 1h). We further examined the on-target editing rates and off-target editing events
189 of each CU-REWIRE variant, and found that these newly engineered variants provide
190 optimal ratios of on- *vs.* off-target editing rates, which may offer versatile options for
191 base editing applications (Fig.1i).

192

193 Like the original CU-REWIREs, the modified CU-REWIRE4 variants
194 predominantly edited cytidines within the UC motif (Supplementary Fig. 2a), reflecting
195 the intrinsic target preference of APOBEC3A [13,27]. To broaden the application scope of
196 RNA base editing, we explored whether the APOBEC-derived base editors can achieve
197 C-to-U editing in other context (i.e., CC, GC, and AC motifs) by systematically
198 screening different AID/APOBEC enzymes that are integrated in the CU-REWIRE
199 platform (Supplementary Fig. 2b). We found that only the APOBEC3A-ePUF10
200 configuration showed detectable base editing near the ePUF10 binding site
201 (Supplementary Fig. 2c), and therefore select APOBEC3A as the chassis to introduce
202 additional modifications that may expand the editing capabilities of new generation
203 CU-REWIREs.

204

205 **AI-Assisted Engineering of Professional APOBECs (ProAPOBECs)**

206 Our analysis of AID/APOBEC proteins revealed that while the deaminase domain is
207 relatively conserved, the NTD and CTD are prone to evolutionary changes [39-41]. This
208 implies that the deaminase domain is crucial for catalyzing the C-to-U transition, while

209 the NTD and CTD may specialize in recognizing different DNA/RNA targets [39].
210 Consistent with this notion, previous studies suggested that various APOBEC proteins
211 might exhibit C-to-U activity outside of the UC context [13], leading us to hypothesize
212 that the core deaminase domain of APOBEC proteins may potentially edit cytosine in
213 diverse contexts when combined with distinct NTD or CTD domains.

214

215 To test this hypothesis, we utilized AlphaFold2 to analyze the structures of
216 APOBEC3 and APOBEC1 from both human and rodent origins (Fig. 2a), similar to a
217 previously used approach that analyzes deaminases across different species [43]. These
218 two enzymes are the only cytosine deaminases that are currently effective as active
219 domains in DNA and RNA base editors [13]. We analyzed the phylogenetic tree of
220 AID/APOBEC family using 1160 full length eukaryotic AID/APOBEC-related genes
221 documented in the NCBI database, and found that the APOBEC3 and APOBEC1
222 belong to the closely related clade of this tree (Fig. 2b). There is striking similarity in
223 the core deaminase domains of APOBEC3s and APOBEC1s, suggesting that functional
224 modules may be interchangeable among these proteins. Therefore we combined the
225 core deaminase domain of different APOBECs with the NTD and CTD of human
226 APOBEC3A. These hybrid deaminases were termed ProAPOBECs, potentially
227 applicable for both DNA and RNA base editing (Fig. 2c). Together, over thousands of
228 functional ProAPOBEC proteins could be predicted (Fig. 2d).

229

We then applied AlphaFold2 to predict structures of ProAPOBECs derived from human and rodent deaminase domains (Fig. 2e and Supplementary Fig. 2d). These ProAPOBECs showed structural conservation with human APOBEC3A, suggesting their potential functionality for base editing. We subsequently fused various ProAPOBECs-C171A with the ePUF10 domain, creating a new generation of CU-REWIREs (version 5.1 to 5.17) (Fig. 2f,g and Supplementary Table 1). Upon expression analysis, most of the CU-REWIRE5 variants (CU5s) demonstrated stable expression and various editing activity towards C_{459} site of EGFP mRNA expressed in the HEK293T cells (Fig. 2h,i). This result demonstrated that we have significantly expanded the AID/APOBEC protein repertoire, leading to the development of novel RNA base editors with a broader targeting context for C-to-U editing. Next, we aim to characterize the editing properties and specificities of these newly engineered CU5s in additional target sites.

Enhanced Targeting Range and Specificity in RNA Base Editing with CU5s Toolkit

We evaluated the RNA editing activity of CU5s by testing their C-to-U editing capabilities at the artificially modified sites of EGFP mRNA, where the $U_{458}\underline{C}_{459}$ was altered to G<u>C</u>, C<u>C</u>, and A<u>C</u> to test the sequence preference of CU5s (Fig. 3a). Surprisingly, multiple CU5s base editor containing ProAPOBECs exhibited C-to-U transition under G<u>C</u>, C<u>C</u>, and A<u>C</u> contexts (Fig. 3b). We found that while some new enzymes (like CU5.7 and 5.13) maintain the original preference of U<u>C</u> context for their editing activity (Fig. 3b and Supplementary Fig. 3a,b). The CU5.16, which demonstrates a particular interest in the novel C-to-U editors with A<u>C</u> context

(Supplementary Fig. 3c-f).

Importantly, new CU5s have high sequence specificity distinct from the original UC specificity [21,27]. For example, the CU5.1 and 5.8, containing the deaminase domain of human APOBEC1 and APOBEC3H respectively, demonstrated significant C-to-U editing activity within GC or AC motifs (Fig. 3b and Supplementary Fig. 4a,b). Our finding underscores that Pro.hAPOBEC1 editing capabilities significantly differ from natural human APOBEC 3A (only editing UC motifs) and human APOBEC1 (editing UC motifs with low efficiency), indicating the emergence of novel cytidine editing activities in engineered ProAPOBECs. In addition, the CU5.15, containing the deaminase domain of mouse APOBEC3, demonstrated significant C-to-U editing activity within CC or UC motifs (Fig. 3b and Supplementary Fig. 4c). The other enzymes can edit cytosine at various sequence context, including two enzymes (CU5.3 and 5.17, containing the deaminase domain of mouse APOBEC1 and rat APOBEC1 respectively.) that can edit the cytosine in any context (i.e., NC motifs), suggesting they may function as a base editor with broad target range (Fig. 3b and Supplementary Fig. 4d,e). Such expansion of specificity is particularly useful in their application as a therapeutic protein (Fig. 3b, Supplementary Fig. 3 and 4).

We further used RNA-seq to assess the bystander editing effects of these new CU5s, with particular interest in the novel C-to-U editors with different sequence specificity (like GC editors CU5.1 and 5.8 (Fig. 3c, top), the CC editor CU5.15 (Fig. 3c, middle), and the NC editors CU5.3 and 5.17 (Fig. 3c, below).

The RNA-seq experiments also allow us to assess the global off-target effects of

278 CU5s across the entire transcriptome (Fig. 3d). Our results demonstrated that the CU5.1,
279 5.17, and 5.16 showed higher off-targeting editing rates compared to CU4.1, while
280 certain CU5s have lower number of off-target editing sites (Fig. 3d). There seems to be
281 correlation between off-target editing rates and the on-target editing efficiency (i.e.,
282 more activity CU5s have a larger number of off-target edit sites), suggesting that we
283 have to balance these two properties of CU5s in the practical applications. We further
284 analyzed the off-target editing sites for their consensus sequence motifs (Fig. 3e), and
285 found that these motifs are largely consistent with the sequence preference observed
286 using C-to-U editing on a single target site (C_{459}) of EGFP mRNA (Fig. 3b and
287 Supplementary Fig. 4).

288

289 **Editing Windows and *in vitro* Application of CU5s**

290 To elucidate the editing characteristics of CU5s on the target RNA, we conducted a
291 comprehensive evaluation of the editing windows associated with selected CU5s. Three
292 variants, CU5.1, CU5.15 and CU5.17, were selected for this analysis, because they can
293 edit cytosine in the new sequence context other that the original U<u>C</u> motifs. We found
294 that CU5.1 (editing at G<u>C</u> motif) demonstrated the highest editing efficiency at
295 positions 2- or 4-nucleotides (nt) downstream of the ePUF10 binding site in EGFP
296 mRNA, as shown by different target reporters containing G<u>C</u> dinucleotides at different
297 positions downstream of the ePUF10 binding site (Fig. 4a).

298

299 We further evaluated the efficacy of CU5.1 in reporter genes carrying disease-
300 causing mutations. For instance, the T143C mutation in the *SOD1* allele, which results

in the p.V48A substitution in the SOD1 protein, is the most common mutation associated with ALS in Southeastern China [44]. We designed two CU5.1 enzymes with ePUF10 domains targeting sequences at positions U_{132}–U_{141} and A_{131}–A_{140} (i.e., 2 or 3 nucleotides upstream of C_{143}, respectively). The CU5.1 enzyme binding 2 nucleotides upstream of the mutated site successfully converted C_{143} to U_{143} with an editing efficiency of ~85%, effectively transforming the mutant *SOD1* allele into the benign form [45] (Fig. 4b).

In another example, the T526C mutation in the APOE4 allele, causing p.R176C in APOE4 protein, was found to be associated with Alzheimer's disease [46,47]. We designed CU5.1 binding to the APOE4 sequences, and found that the CU5.1 binding at 2-nt upstream of the mutated site effectively converted C_{526} to U_{526} with editing efficiency at ~90%, potentially transforming APOE4 into the benign APOE1 allele [48] (Fig. 4c). In addition, the c.68C>A (p.P23H) mutation in the human Rhodopsin gene, known to cause Retinitis Pigmentosa (RP) [49] can be effectively edited by CU5.1 that bind to 2-nt upstream of the mutated site (Figure 4c). As a result of editing C_{76} to U_{76}, we introduced a stop codon in the mutated mRNA, which should abolish the toxic protein mutant (Fig. 4d). Combining the results across different target mRNAs, we summarized the editing window for CU5.1 as 2~5-nt downstream of the ePUF10 binding site (Fig. 4e).

Furthermore, CU5.15 demonstrated the highest editing efficiency 2-nt downstream of the ePUF10 binding site in EGFP mRNA (Fig. 4f). We adopted similar approach

323 to examine the editing window of CU5.15 using reporters containing CC at different
324 distance from the designed binding site (Fig. 4f), or using multiple CU5.15 targeting
325 the c.104T>C (p.L35P) mutation in MEF2C gene (Fig. 4g) [8]. We found that CU5.15
326 effectively edited cytidine 2-nt or 3-nt downstream of the ePUF10 binding site,
327 resulting in an editing window within 2~4-nt in various target mRNAs (Fig. 4h).
328
329 Finally, CU5.17, with editing activity in "NC" context, demonstrated a high
330 efficiency at positions 2-nt downstream of the ePUF10 binding site as judged by EGFP
331 reporter (Fig. 4i). Importantly, CU5.17 was highly efficient in editing the T1541C site
332 of the human DDX3X mRNA linked to neurodevelopmental disorders [50], particularly
333 when the CU5.17 binding to 2-nt or 3-nt upstream of the mutated site (Fig. 4j). Although
334 bystander editing at C_{1542} occurred, this did not affect the amino acid sequence of
335 DDX3X (Fig. 4j), indicating the editing window for CU5.17 is within 2~5-nt after the
336 ePUF10 binding site across different mRNAs (Fig. 4k).
337
338 **Improving the CU-REWIRE5 system with AI-Assisted Design of ProAPOBECs**
339 **utilizing cytosine Deaminase derived from Mammals**
340 We also explored the possibility of using ProAPOBECs derived from deaminase of
341 other mammalian species using similar approach (Supplementary Fig. 5 and
342 Supplementary Table 1). AlphaFold2-based predictions revealed that the deaminase
343 domains from many mammalian APOBEC1s and APOBEC3s may form functional
344 structures with the NTD and CTD of the human APOBEC3A (Supplementary Fig. 5a).

345 We found that both Z1 and Z2 domains of mammalian APOBEC3s could form
346 functional ProAPOBECs when combined with NTD and CTD of human APOBEC3A
347 (Supplementary Fig. 5b,c).
348
349 Furthermore, we integrated these newly engineered ProAPOBECs into CU-
350 REWIRE (i.e., by fusing with ePUF10 domain) and tested their editing activity on
351 EGFP mRNA. We found significant C-to-U editing activity in GC, AC, and CC contexts
352 by different ProAPOBECs (Supplementary Fig. 5d,e). ProAPOBECs with deaminase
353 domains from APOBEC1 showed strong activity in GC contexts, while some with
354 APOBEC3-Z1 domains demonstrated activity in CC and AC contexts (Supplementary
355 Fig. 5f-h). These results highlight the versatility of engineered ProAPOBECs for C-to-
356 U base editing, suggesting an expansion of specificity is particularly useful in potential
357 therapeutic applications.
358
359 ***In Vivo* RNA Editing of PCSK9 in Mice reduces cholesterol levels**
360 To demonstrate *in vivo* applications, we applied CU-REWIREs to edit *Pcsk9*, a
361 therapeutic target gene, by introducing a premature stop codon to repress PCSK9
362 protein expression [51]. Inhibiting PCSK9 protein reduces serum low-density lipoprotein
363 cholesterol (LDL-C) levels, which is associated with a lower risk of cardiovascular
364 disease [52]. Our aim was to achieve precise RNA editing of *PCSK9* without alternations
365 of genome DNA, addressing limitations commonly associated with DNA editing
366 strategies [53-55].

First, we assessed the editing efficiency of various CU-REWIREs and the Cas13-based C-to-U editors (CURE [23], xCBE [22]) in generating premature stop codons at the $C_{832}AG$ position within a mouse *Pcsk9* reporter in HEK293T cells (Fig. 5a). While no significant editing was observed with CURE or xCBE, CU4.1 (CU-REWIRE4.1) and CU5-A3Z1-1 (CU-REWIRE5 featuring ProAPOBEC from *Ailuropoda melanoleuca*) effectively converted $C_{832}AG$ to $U_{832}AG$ when ePUF10 domains bound to sequences spanning U_{821}–G_{830} (Fig. 5a). Notably, CU5-A3Z1-1 demonstrated a remarkable 1.6-fold increase in editing efficiency compared to CU4.1, achieving 96% versus 37%, respectively (Fig. 5a). This highlights the superior application potential of ProAPOBEC in specific contexts compared to native APOBEC proteins.

Next, we packaged CU5-A3Z1-1 into an AAV8 delivery system (Fig. 5b), leveraging its high liver tropism for in vivo base editing. Mice injected with CU5-A3Z1-1 were analyzed for changes in *PCSK9* mRNA, protein levels, and total cholesterol four weeks post-administration. By introducing a premature stop codon, the edited *PCSK9* mRNA was subjected to degradation via nonsense-mediated mRNA decay [56]. Quantitative PCR revealed that CU5-A3Z1-1 (2×10^{12} viral genomes (vg)) reduced *PCSK9* mRNA levels by over 70% compared to the EGFP control group (Fig. 5c). Consistently, this led to significant reductions in both PCSK9 protein levels (Fig. 5d) and cholesterol levels (Fig. 5e), without affecting serum glyceride or total protein levels (Fig. 5f,g).

As expected, the mice showed no abnormalities in growth following CU5-A3Z1-1 administration (Fig. 5h). Transcriptome-wide RNA sequencing identified approximately 400 C-to-U editing events associated with CU5-A3Z1-1 treatment (Fig. 5i). These findings demonstrate that CU5-A3Z1-1 enables efficient and precise in vivo editing of *PCSK9*, offering therapeutic benefits with minimal transcriptome-wide off-target effects.

In Vivo **RNA Editing in an ASD Mouse Model Using CU5.15**

Effective RNA base editing in the brain has been a challenging endeavor [20]. To explore the potential of CU5s, powered by ProAPOBECs, for *in vivo* RNA editing, we utilized an ASD mouse model with L35P (c.104T>C) point mutation in MEF2C gene, which was reported to cause severe ASD in human [8]. An APOBEC-embedded cytosine base editor for DNA has successfully performed C-to-T conversion at the C_{104} site of the Mef2c gene in the Mef2c L35P mutant mice, effectively reversing the ASD-like phenotypes in this mouse model [8]. However, the previous methods need to co-inject two AAV vectors for in vivo DNA base editing, posing practical challenges for its application in clinical settings [6,8,57]. Packaging the base editing system into a single AAV vector could significantly reduce costs and enhance delivery efficiency in clinical applications.

We first examined the C-to-U base editing efficiency of the CU-REWIRE system as compared with Cas13-based RNA editing tools on the C_{104} site on the Mouse Mef2c

411 (c.104) mRNA reporter [23,27] (Supplementary Fig. 6). We observed that CU5s exhibited
412 significantly higher editing efficiency compared to CRISPR/Cas-based tools.
413 Specifically, CU5.15 achieved an editing efficiency of 43%, and CU1.15 reached 18%
414 (Supplementary Fig. 6a-b), whereas the CRISPR/Cas-based tool CURE-X-
415 Pro.mAPOBEC3-1 showed only 5% efficiency (Supplementary Fig. 6c-d). Notably, the
416 CURE-X system utilizing native APOBEC proteins failed to edit the target *Mef2c*
417 mRNA. However, replacing the native APOBEC with ProAPOBEC in the CURE-X-
418 Pro.mAPOBEC3-1 system resulted in effective editing (Supplementary Fig. 6c-e),
419 underscoring the therapeutic potential of ProAPOBECs in Cas13-based RNA base
420 editors.
421
422 We further packaged CU5.15, featuring the ePUF10 module targeting the A_{92}-A_{101}
423 region of mouse Mef2c mRNA, into brain blood barrier (BBB)-crossing AAV-PHP.eB
424 vectors (Fig. 6a). These vectors, along with an EGFP reporter driven by the human
425 synapsin 1 gene promoter (hSyn), were injected into the tail vein of 4-week-old Mef2c
426 WT and L35P$^{+/-}$ mice [8]. Robust EGFP expression was observed in the cortical and
427 hippocampal regions 4- and 16- weeks post-injection (Fig. 6b, c), confirming the
428 efficient gene delivery in brains.
429
430 Sanger sequencing and RNA-sequencing of prefrontal cortical and hippocampus
431 tissue samples from the mice revealed that CU5.15 induced C-to-U editing at the C_{104}
432 site in the Mef2c L35P$^{+/-}$ mice injected with CU5.15 (Supplementary Fig. 7). RNA-seq

experiments showed a significant increase in the percentage of U_{104} in the prefrontal cortex (61.3%) and hippocampus (68%) of Mef2c L35P$^{+/-}$ mice injected with CU5.15, compared to those injected with ePUF10 (Fig. 6d,e). This data confirmed the induction of C-to-U editing events by CU5.15. Additionally, no bystander editing events were observed in the C nucleotides from positions C_{65}-C_{150} of Mef2c mRNA, demonstrating the precision of CU5.15-mediated RNA editing (Figure 6d). C-to-U editing rates across various brain regions ranged from 30-50% (Fig. 6e). Considering that the brain tissues collected for RNA-seq are mixture of neurons and glial cells, the exact C-to-U editing of the Mef2c L35P site in neurons would be higher. Transcriptome-wide RNA sequencing revealed approximately 800 C-to-U editing events associated with CU5.15 (Fig. 6f).

Notably, MEF2C protein levels were fully restored in the cortical and hippocampal regions of Mef2c L35P$^{+/-}$ mice injected with CU5.15, as compared to those injected with ePUF10 and to Mef2c WT mice (Fig. 6g). This restoration was further validated by immunostaining using an anti-MEF2C antibody (Fig. 7a,b). Remarkably, the lifespans of Mef2c L35P$^{+/-}$ mice injected with CU5.15 were close to WT group (Fig. 7c), which was not observed in previous DNA editing work [8], suggesting that RNA base editing facilitated by CU5.15 may exert a broader impact in this mouse model.

We subsequently examined the influence of CU5.15 on autistic-like behaviors in Mef2c L35P mice using a series of social interaction tests. The investigation began with

the three-chamber test, comprising both sociability and social novelty tests. In the sociability test, mice were given the choice between interacting with another mouse or an empty cage (Fig. 7d). This was followed by the social novelty test, where the mice had to choose between a familiar partner and a novel partner. Mice treated with AAV-CU5.15 demonstrated a significant improvement in social interaction performance during the social novelty test [8] (Fig. 7e,f).

The study progressed to analyzing social interaction behaviors using the social intruder test, consisting of six trials (T0-T5) (Fig. 7g). After three days of social isolation (T0), the mice encountered the same partner for four consecutive trials (T1-T4, each lasting 5 minutes), and then a new partner in the fifth trial (T5). The duration of sniffing time between the subject mice and their partners was recorded. Notably, the aberrant social behaviors observed in Mef2c L35P mice during the initial four trials (T1-T4) with intruder partners were entirely mitigated following treatment with CU5.15 (Fig. 7g-j). These findings suggest that in vivo RNA base editing facilitated by CU5.15 effectively restores normal MEF2C protein expression and alleviates the social impairments associated with the Mef2c L35P mutation.

In summary, our study demonstrates that RNA base editing, as facilitated by CU5.15, provides a potent tool for correcting genetic mutations in the brain and has potential therapeutic applications for ASD and other genetic disorders.

Discussion

APOBEC3A is a highly active deaminase frequently used in DNA base editors. However, its application has been hindered by some intrinsic limitations of this enzyme, including off-target effects and RNA binding issues [11,12]. Although point mutations in APOBEC3A have reduced off-target effects in DNA base editing, its application in RNA base editing has remained largely unexplored [58,59]. We hypothesized that the high off-targeting rates of APOBEC3A might be largely due to its close interaction with target mRNA. Structurally, the dimerization of APOBEC3A plays a key role in stabilizing its mRNA binding. Therefore, our initial strategy was to modulate dimerization to minimize its off-target effects and decrease the strong associations with mRNA. Indeed, APOBEC3A mutants in the NTD or CTD, exhibiting reduced mRNA interaction and dimerization, showed fewer off-target effects. This provided a range of APOBEC3A variants for precise RNA base editing in conjunction with the REWIRE system (Fig. 1c-i). However, such variants were limited to editing cytidines in UC contexts (Supplementary Fig. 2a), indicating the need for a more fundamental protein engineering of cytosine base editors with broader targeting scopes.

Utilizing AlphaFold2-assisted protein structure analysis, we discovered that the deaminase domains of APOBECs could act as interchangeable modules (Fig. 2). This suggested that the NTD and CTD may contribute to the recognition of viral genetic materials in various organisms. Consequently, we anticipated that novel deaminase activities could emerge from new combinations of deaminases with NTDs and CTDs.

499 This led to the identification of a series of APOBECs with novel cytidine-editing
500 activity under various contexts, significantly broadening the application of REWIRE-
501 mediated RNA base editing.
502
503 Compared to Cas13-based C-to-U base editors, the CU5s with installed
504 ProAPOBECs demonstrated an impressive capacity for effecting C-to-U transitions.
505 Notably, our study revealed that the CU 5.7 and 5.13 are capable of editing cytosine in
506 UC motifs, akin to the CasR13-based RNA editing system that utilizes human
507 APOBEC3A or evolved ADAR2 enzyme [21,23], the CU5.15 enzyme can edit cytosine
508 across CC sequence context, similar to the SNAP-CDAR-S system that employs a
509 evolved ADAR2 enzyme [24] . Meanwhile, the CU5.3 and 5.17 enzyme can edit cytosine
510 across NC sequence context, suggesting their potential as broad-spectrum editing tools.
511 Importantly, multiple CU5s base editor have shown remarkable C-to-U transitions
512 capabilities within GC, AC, and CC motifs, exhibiting high sequence specificity distinct
513 from traditional RNA base editors (Fig. 3). For example, CU5.1 has shown significant
514 C-to-U editing activity within GC motifs, albeit with lower efficiency in AC motifs.
515 This enzyme notably reduces bystander editing effects and enhances editing specificity
516 in the target region. Such expansion of specificity is particularly useful in their
517 application as a therapeutic protein (Fig. 3, Supplementary Fig. 3 and 4).
518
519 While Cas13-mediated A-to-I RNA editing has been reported in mouse models of
520 human genetic disorders [18,20], effective C- to-U RNA editing had not been achieved due

521 to the intrinsic properties of APOBECs. With the new REWIRE system, we
522 demonstrated that ProAPOBEC can effectively perform RNA base editing in the liver
523 and brain (Fig. 5,6). With an editing rate of nearly 50% *in vivo*, Mef2c mutant mice
524 showed restored protein levels and correction of autistic-like behaviors. Furthermore,
525 effective RNA base editing prolonged the lifespan of Mef2c mutant mice, a result not
526 observed with the Mef2c L35P DNA editing [8]. The effects of *in vivo* RNA base editing
527 in our study appear to be long-lasting for over 6 months (Fig. 7c).
528
529 ProAPOBECs also have potential applications in the field of RNA epigenetics. The
530 elucidation of epigenetic modifications in DNA and RNA has become crucial for
531 understanding their diverse biological functions [60]. RNA modifications add a new layer
532 to gene regulation, giving rise to "RNA epigenetics." Techniques such as DART-seq
533 (deamination adjacent to RNA modification targets) [61], ACE-Seq (APOBEC-coupled
534 epigenetic sequencing) [62], and AMD-Seq (APOBEC3A-mediated deamination
535 sequencing) [63], all employing APOBECs manipulation, have been developed for
536 comprehensive mapping of RNA epigenetics. Additionally, RNA-binding proteins
537 (RBPs) are pivotal in gene expression and RNA processing. To elucidate RBP dynamics
538 at the single-cell level, the Gene lab developed STAMP (Surveying Targets by
539 APOBEC-Mediated Profiling), enhancing the detection of RBP-RNA interactions [64].
540
541 The ProAPOBECs engineered in this study have enhanced editing efficiency and
542 specificity over their natural APOBEC counterparts, emerging as significant

improvement to the current repertoire of tools available for genetic modification. Our objective is to refine the ProAPOBECs' activity and expand their application, facilitating the development of streamlined and accurate methods for conducting both DNA and RNA edits in vivo. In summary, the integration of REWIRE technology with ProAPOBEC-mediated base editing heralds a promising new era in both fundamental research and applied therapeutic strategies. This work not only enriches the existing collection of tools for genetic engineering but also paves the way for novel approaches to treat and manage genetic disorders, marking a significant step forward in the field of genomics and molecular medicine.

Acknowledgments

We extend our gratitude to Dr. Li Yang of Fudan University for the gift of native human/mouse APOBECs, to Dr. Tian Chi of ShanghaiTech University for the CURE plasmids, and to Dr. Chunlong Xu of Lingang Laboratory for the xCBE plasmids. This work is supported by Fundamental Research Funds for the Central Universities (Z.Q), NSFC grants (82430046 to Z.Q., 32030064 to Z.W., 82201632 to W.H.); Project of Medical Technology Research and Transformation supported by Shanghai Municipal Health Commission (2024ZZ1007) (Z.Q.); the National Key Research and Development Program of China (2021YFA1300503), the Starry Night Science Fund at Shanghai Institute for Advanced Study of Zhejiang University (SN-ZJU-SIAS-009) (Z.W.). W.H. is supported by the Fellowship of China Postdoctoral Science Foundation (2022M723244) and the Shanghai Postdoctoral Excellence Program (2022777).

Author contributions statement

Conceptualization, W.H., Z.Q., Z.W.; Biochemical and cell culture experiments, W.H.; NGS data analysis, B.Y.; AI-Assisted protein structure predictions, X.F., M.H.; Animal experiments, W.H., W.L., Y.Y., Y.Z., S.W. and S.S.; Writing, W.H., Z.W. and Z.Q.

Data and code availability

The original RNA sequencing datasets have been deposited in the NCBI Gene Expression Omnibus (accession code PRJNA1068267). Custom computer code is available upon request. Accession numbers of RNA-seq data are provided in Table S2.

Competing interests:

Authors declare no competing interests.

Reference

1 Rees, H. A. & Liu, D. R. Base editing: precision chemistry on the genome and transcriptome of living cells. *Nat Rev Genet* **19**, 770-788 (2018). https://doi.org:10.1038/s41576-018-0059-1

2 Porto, E. M., Komor, A. C., Slaymaker, I. M. & Yeo, G. W. Base editing: advances and therapeutic opportunities. *Nat Rev Drug Discov* **19**, 839-859 (2020). https://doi.org:10.1038/s41573-020-0084-6

3 Komor, A. C., Kim, Y. B., Packer, M. S., Zuris, J. A. & Liu, D. R. Programmable editing of a target base in genomic DNA without double-stranded DNA cleavage. *Nature* **533**, 420-424 (2016). https://doi.org:10.1038/nature17946

4 Nishida, K. *et al.* Targeted nucleotide editing using hybrid prokaryotic and vertebrate adaptive immune systems. *Science* **353**, aaf8727 (2016). https://doi.org:10.1126/science.aaf8729

5 Gaudelli, N. M. *et al.* Programmable base editing of A*T to G*C in genomic DNA without DNA cleavage. *Nature* **551**, 464-471 (2017). https://doi.org:10.1038/nature24644

6 Koblan, L. W. *et al.* In vivo base editing rescues Hutchinson-Gilford progeria syndrome in mice. *Nature* **589**, 608-614 (2021). https://doi.org:10.1038/s41586-020-03086-7

7 Mandana Arbab, Z. M., Kaitlyn M. Kray, Ailing Du, Gregory A. Newby, Anton J. Blatnik, Aditya Raguram, Michelle F. Richter, Kevin T. Zhao, Jonathan M. Levy, Max W. Shen, W. David Arnold, Dan Wang, Jun Xie, Guangping Gao, Arthur H. M. Burghes, David R. Liu. Base editing rescue of spinal muscular atrophy in cells and in mice. *science* **380** (2023). https://doi.org:doi: 10.1126/science.adg6518.

8 Li, W. K. *et al.* Whole-brain in vivo base editing reverses behavioral changes in Mef2c-mutant mice. *Nat Neurosci* **27**, 116-128 (2024). https://doi.org:10.1038/s41593-023-01499-x

9 Wang, X. *et al.* Efficient base editing in methylated regions with a human APOBEC3A-Cas9 fusion. *Nat Biotechnol* **36**, 946-949 (2018). https://doi.org:10.1038/nbt.4198

10 Kim, D. *et al.* Genome-wide target specificities of CRISPR RNA-guided programmable deaminases. *Nat Biotechnol* **35**, 475-480 (2017). https://doi.org:10.1038/nbt.3852

11 Erwei Zuo, Y. S., Wu Wei, Tanglong Yuan, Wenqin Ying, Hao Sun, Liyun Yuan, Lars M. Steinmetz, Yixue Li, Hui Yang. Cytosine base editor generates substantial off-target single nucleotide variants in mouse embryos. *science* **364**, 289–292 (2019). https://doi.org:10.1126/science.aav9973

12 Shuai Jin et al. Cytosine, but not adenine, base editors induce genome-wide off-target mutations in rice. *Science* **364**, 292–295 (2019). https://doi.org:10.1126/science.aaw7166

13 Pecori, R., Di Giorgio, S., Paulo Lorenzo, J. & Nina Papavasiliou, F. Functions and consequences of AID/APOBEC-mediated DNA and RNA deamination. *Nat Rev Genet* **23**, 505-518 (2022). https://doi.org:10.1038/s41576-022-00459-8

14 Stafforst, T., Schneider, M. F. An RNA-deaminase conjugate selectively repairs point mutations. *Angew Chem Int Ed Engl* **51**, 11166-11169 (2012). https://doi.org:10.1002/anie.201206489

15 David B.T. Cox, J. S. G., Omar O. Abudayyeh, Brian Franklin,Max J. Kellner,Julia Joung, Feng Zhang. RNA editing with CRISPR-Cas13. *Science* **358**, 1019-1027 (2017). https://doi.org:DOI: 10.1126/science.aaq0180

16 Vogel, P. *et al.* Efficient and precise editing of endogenous transcripts with SNAP-tagged ADARs. *Nat Methods* **15**, 535-538 (2018). https://doi.org:10.1038/s41592-018-0017-z

17 Katrekar, D. *et al.* In vivo RNA editing of point mutations via RNA-guided adenosine deaminases. *Nat Methods* **16**, 239-242 (2019). https://doi.org:10.1038/s41592-019-0323-0

18 Qingquan Xiao, Z. X., Yuanyuan Xue, Chunlong Xu, Lei Han, Yuanhua Liu, Fang Wang, Runze Zhang, Shuang Han, Xing Wang, Geng-Lin Li, Huawei Li, Hui Yang, Yilai Shu. Rescue of autosomal dominant hearing loss by in vivo delivery of mini dCas13X-derived RNA base editor. *Sci Transl Med* **14** (2022). https://doi.org:10.1126/scitranslmed.abn0449

19 Yi, Z. *et al.* Engineered circular ADAR-recruiting RNAs increase the efficiency and fidelity of RNA editing in vitro and in vivo. *Nat Biotechnol* **40**, 946-955 (2022). https://doi.org:10.1038/s41587-021-01180-3

20 Sinnamon, J. R. *et al.* Targeted RNA editing in brainstem alleviates respiratory dysfunction in a mouse model of Rett syndrome. *Proc Natl Acad Sci U S A* **119**, e2206053119 (2022). https://doi.org:10.1073/pnas.2206053119

21 Omar O Abudayyeh, J. S. G., Brian Franklin, Jeremy Koob, Max J Kellner, Alim Ladha, Julia Joung, Paul Kirchgatterer, David B T Cox, Feng Zhang. A cytosine deaminase for programmable single-base RNA editing. *Science* **353**, aaf5573 (2019). https://doi.org:10.1126/science.aaf5573

22 Xu, C. *et al.* Programmable RNA editing with compact CRISPR-Cas13 systems from uncultivated microbes. *Nat Methods* **18**, 499-506 (2021). https://doi.org:10.1038/s41592-021-01124-4

23 Huang, X. *et al.* Programmable C-to-U RNA editing using the human APOBEC3A deaminase. *EMBO J* **39**, e104741 (2020). https://doi.org:10.15252/embj.2020104741

24 Latifi, N., Mack, A. M., Tellioglu, I., Di Giorgio, S. & Stafforst, T. Precise and efficient C-to-U RNA base editing with SNAP-CDAR-S. *Nucleic Acids Res* **51**, e84 (2023). https://doi.org:10.1093/nar/gkad598

25 Stroppel, A. S. *et al.* Harnessing self-labeling enzymes for selective and concurrent A-to-I and C-to-U RNA base editing. *Nucleic Acids Res* **49**, e95 (2021). https://doi.org:10.1093/nar/gkab541

26 Salter, J. D., Bennett, R. P. & Smith, H. C. The APOBEC Protein Family: United by Structure, Divergent in Function. *Trends Biochem Sci* **41**, 578-594 (2016). https://doi.org:10.1016/j.tibs.2016.05.001

27 Han, W. *et al.* Programmable RNA base editing with a single gRNA-free enzyme. *Nucleic Acids Res* **50**, 9580–9595 (2022). https://doi.org:10.1093/nar/gkac713

28 Hall, C.-G. C. a. T. M. T. Engineering RNA sequence specificity of Pumilio repeats. *Proc Natl Acad Sci USA* **103**, 13635–13639 (2006). https://doi.org:10.1073 pnas.0606294103

29 Dong, S. *et al.* Specific and modular binding code for cytosine recognition in Pumilio/FBF (PUF) RNA-binding domains. *J Biol Chem* **286**, 26732-26742 (2011). https://doi.org:10.1074/jbc.M111.244889

30 Filipovska, A., Razif, M. F., Nygard, K. K. & Rackham, O. A universal code for RNA recognition by PUF proteins. *Nat Chem Biol* **7**, 425-427 (2011). https://doi.org:10.1038/nchembio.577

31 Zhao, Y. Y. *et al.* Expanding RNA binding specificity and affinity of engineered PUF domains. *Nucleic Acids Res* **46**, 4771-4782 (2018). https://doi.org:10.1093/nar/gky134

32 Jarmoskaite, I. *et al.* A Quantitative and Predictive Model for RNA Binding by Human Pumilio Proteins. *Mol Cell* **74**, 966-981 e918 (2019). https://doi.org:10.1016/j.molcel.2019.04.012

33 Wang, Y., Cheong, C. G., Hall, T. M. & Wang, Z. Engineering splicing factors with designed specificities. *Nat Methods* **6**, 825-830 (2009). https://doi.org:10.1038/nmeth.1379

34 Cooke, A., Prigge, A., Opperman, L. & Wickens, M. Targeted translational regulation using the PUF protein family scaffold. *Proc Natl Acad Sci U S A* **108**, 15870-15875 (2011). https://doi.org:10.1073/pnas.1105151108

35 Choudhury, R., Tsai, Y. S., Dominguez, D., Wang, Y. & Wang, Z. Engineering RNA endonucleases with customized sequence specificities. *Nat Commun* **3**, 1147 (2012). https://doi.org:10.1038/ncomms2154

36 Shinoda, K., Suda, A., Otonari, K., Futaki, S. & Imanishi, M. Programmable RNA methylation and demethylation using PUF RNA binding proteins. *Chem Commun (Camb)* **56**, 1365-1368 (2020). https://doi.org:10.1039/c9cc09298f

37 Gough, V. & Gersbach, C. A. Immunity to Cas9 as an Obstacle to Persistent Genome Editing. *Mol Ther* **28**, 1389-1391 (2020). https://doi.org:10.1016/j.ymthe.2020.05.007

38 Bohn, M. F. *et al.* The ssDNA Mutator APOBEC3A Is Regulated by Cooperative Dimerization. *Structure* **23**, 903-911 (2015). https://doi.org:10.1016/j.str.2015.03.016

39 Ito, J., Gifford, R. J. & Sato, K. Retroviruses drive the rapid evolution of mammalian APOBEC3 genes. *Proc Natl Acad Sci USA* **117**, 610-618 (2020). https://doi.org:10.1073/pnas.1914183116

40 Conticello, S. G., Thomas, C. J., Petersen-Mahrt, S. K. & Neuberger, M. S. Evolution of the AID/APOBEC family of polynucleotide (deoxy)cytidine deaminases. *Mol Biol Evol* **22**, 367-377 (2005). https://doi.org:10.1093/molbev/msi026

41 Wenqiang Wang, G.-Z. H. A Long-Running Arms Race between APOBEC1 Genes and Retroviruses in Tetrapods. *Journal of Virology* **97** (2023). https://doi.org:10.1128/jvi.01795-22

42 Lu, G. & Hall, T. M. Alternate modes of cognate RNA recognition by human PUMILIO proteins. *Structure* **19**, 361-367 (2011). https://doi.org:10.1016/j.str.2010.12.019

43 Huang, J. *et al.* Discovery of deaminase functions by structure-based protein clustering. *Cell* **186**, 3182-3195 e3114 (2023). https://doi.org:10.1016/j.cell.2023.05.041

44 Chen, L. X. *et al.* SOD1 Mutation Spectrum and Natural History of ALS Patients in a 15-Year Cohort in Southeastern China. *Front Genet* **12**, 746060 (2021). https://doi.org:10.3389/fgene.2021.746060

45 Wang, P. S. *et al.* Clinical characterization and founder effect analysis in Chinese amyotrophic lateral sclerosis patients with SOD1 common variants. *Ann Med* **56**, 2407522 (2024). https://doi.org:10.1080/07853890.2024.2407522

46 E. H. Corder, A. M. S., W. J. Strittmatter, D. E. Schmechel, P. C. Gaskell, G. W. Small, A. D. Roses, J. L. Haines and M. A. Gene Dose of Apolipoprotein E Type 4 Allele and the Risk of Alzheimer's Disease in Late Onset Families. *Science* **261**, 921-923 (1993). https://doi.org:10.1126/science.8346443.

47 Blanchard, J. W. *et al.* APOE4 impairs myelination via cholesterol dysregulation in oligodendrocytes. *Nature* **611**, 769-779 (2022). https://doi.org:10.1038/s41586-022-05439-w

48 Ordovas, J. M., Litwack-Klein, L., Wilson, P. W., Schaefer, M. M. & Schaefer, E. J. Apolipoprotein E isoform phenotyping methodology and population frequency with identification of apoE1 and apoE5 isoforms. *Journal of Lipid Research* **28**, 371-380 (1987). https://doi.org:10.1016/s0022-2275(20)38690-9

49 Thaddeus P. Dryja, T. M., Elias Reichel, Lauri B. Hahn, GlennS. Cowley, David W. Yandell, Michael A. Sandberg & Eliot L. Berson*. A point mutation of the rhodopsin gene in one form of retinitis pigmentosa. *Nature* **343**, 364–366 (1990). https://doi.org:10.1038/343364a0

50 Lennox, A. L. *et al.* Pathogenic DDX3X Mutations Impair RNA Metabolism and Neurogenesis during Fetal Cortical Development. *Neuron* **106**, 404-420 e408 (2020). https://doi.org:10.1016/j.neuron.2020.01.042

51 Wang, L. *et al.* Eliminating base-editor-induced genome-wide and transcriptome-wide off-target mutations. *Nat Cell Biol* **23**, 552-563 (2021). https://doi.org:10.1038/s41556-021-00671-4

52 Horton, J. D., Cohen, J. C. & Hobbs, H. H. Molecular biology of PCSK9: its role in LDL metabolism. *Trends Biochem Sci* **32**, 71-77 (2007). https://doi.org:10.1016/j.tibs.2006.12.008

53 Rothgangl, T. *et al.* In vivo adenine base editing of PCSK9 in macaques reduces LDL cholesterol levels. *Nat Biotechnol* **39**, 949-957 (2021). https://doi.org:10.1038/s41587-021-00933-4

54 Musunuru, K. *et al.* In vivo CRISPR base editing of PCSK9 durably lowers cholesterol in primates. *Nature* **593**, 429-434 (2021). https://doi.org:10.1038/s41586-021-03534-y

55 Ran, F. A. *et al.* In vivo genome editing using Staphylococcus aureus Cas9. *Nature* **520**, 186-191 (2015). https://doi.org:10.1038/nature14299

56 Lykke-Andersen, S. & Jensen, T. H. Nonsense-mediated mRNA decay: an intricate machinery that shapes transcriptomes. *Nat Rev Mol Cell Biol* **16**, 665-677 (2015). https://doi.org:10.1038/nrm4063

57 Qi M, M. S., Liu J, Liu X, Wei J, Lu WJ, Zhang S, Chang Y, Zhang Y, Zhong K, Yan Y, Zhu M, Song Y, Chen Y, Hao G, Wang J, Wang L, Lee AS, Chen X, Wang Y, Lan F. . In Vivo Base Editing of Scn5a Rescues Type 3 Long QT Syndrome in Mice. *Circulation* **149**, 317-329 (2024). https://doi.org:10.1161/CIRCULATIONAHA.123.065624

58 Zhou, C. *et al.* Off-target RNA mutation induced by DNA base editing and its elimination by mutagenesis. *Nature* **571**, 275-278 (2019). https://doi.org:10.1038/s41586-019-1314-0

59 Grunewald, J. *et al.* Transcriptome-wide off-target RNA editing induced by CRISPR-guided DNA base editors. *Nature* **569**, 433-437 (2019). https://doi.org:10.1038/s41586-019-1161-z

60 Zhao, L. Y., Song, J., Liu, Y., Song, C. X. & Yi, C. Mapping the epigenetic modifications of DNA and RNA. *Protein Cell* **11**, 792-808 (2020). https://doi.org:10.1007/s13238-020-00733-7

61 Meyer, K. D. DART-seq: an antibody-free method for global m(6)A detection. *Nat Methods* **16**, 1275-1280 (2019). https://doi.org:10.1038/s41592-019-0570-0

62 Emily K Schutsky, J. E. D., Peng Hu, Monica Yun Liu, Christopher S Nabel, Emily B Fabyanic, Young Hwang, Frederic D Bushman, Hao Wu & Rahul M Kohli. Nondestructive, base-resolution sequencing of 5-hydroxymethylcytosine using a DNA deaminase. *Bature Biotechnology* **36**, 1083–1090 (2018). https://doi.org:10.1038/nbt.42041084

63 Li, Q. Y., Xie, N. B., Xiong, J., Yuan, B. F. & Feng, Y. Q. Single-Nucleotide Resolution Analysis of 5-Hydroxymethylcytosine in DNA by Enzyme-Mediated Deamination in Combination with Sequencing. *Anal Chem* **90**, 14622-14628 (2018). https://doi.org:10.1021/acs.analchem.8b04833

64 Brannan, K. W. *et al.* Robust single-cell discovery of RNA targets of RNA-binding proteins and ribosomes. *Nat Methods* **18**, 507-519 (2021). https://doi.org:10.1038/s41592-021-01128-0

Figure legends

Figure 1

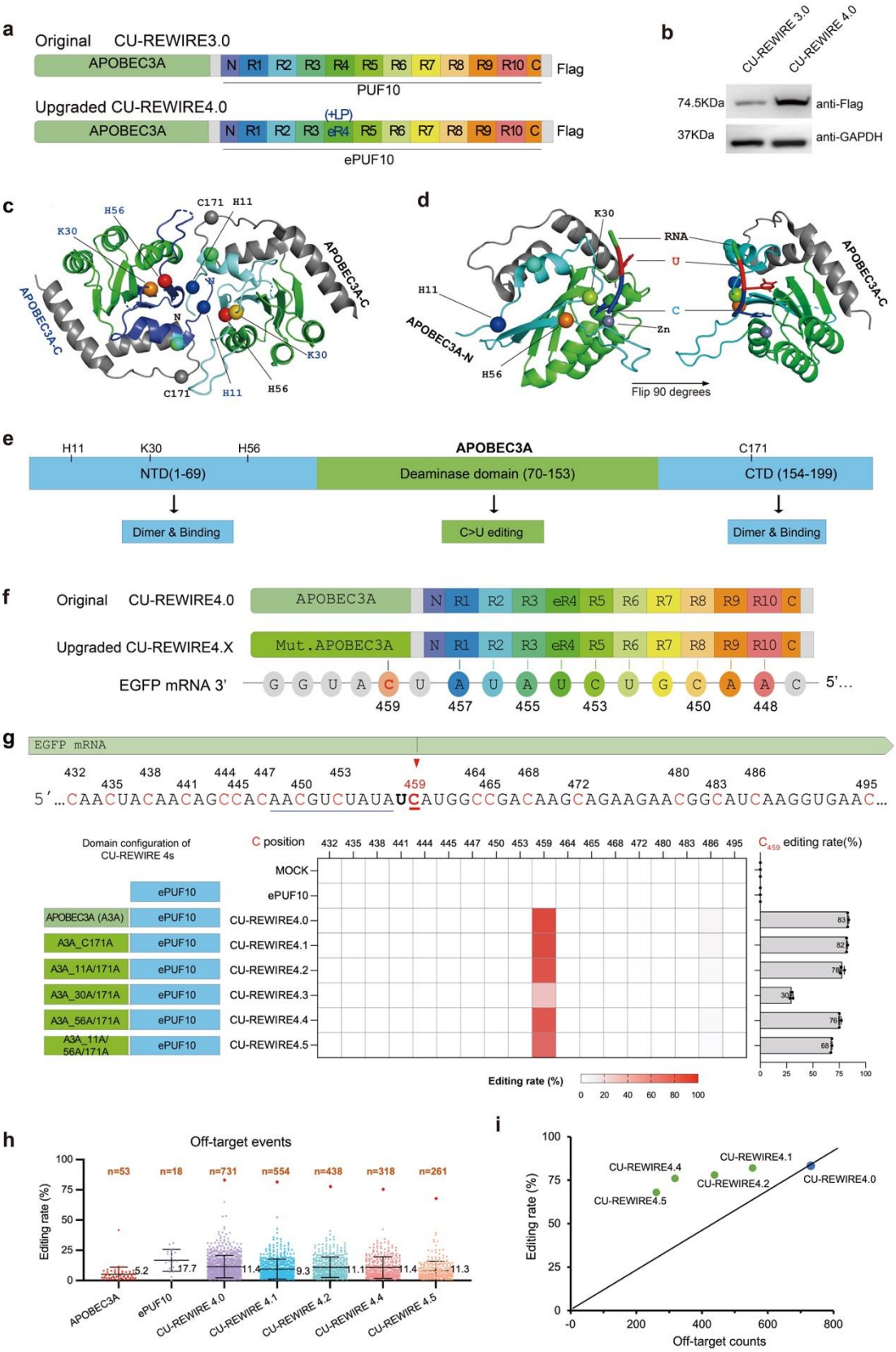

Fig. 1| Structure-based optimization of APOBEC3A enhances editing efficacy and

759 **reduces off-target effects of REWIRE-mediated RNA base editing.**

760 **a,** Schematic design of REWIREs with PUF variants. Top: Original CU-REWIRE 3.0
761 with PUF10, targeting 10-nt sequences. Bottom: Upgraded CU-REWIRE 4.0 with
762 ePUF10.

763 **b,** Expression levels of CU-REWIREs in cultured cells. Representative Western blot
764 images using anti-Flag antibody, related to Supplementary Fig. 1**b**.

765 **c,** Crystal structure of Human APOBEC3A (PDB: 4XXO) highlighting putative
766 dimerization interactions. Amino acids involved in dimer formation are shown in
767 spherical forms.

768 **d,** Crystal structure of Human APOBEC3A (PDB: 5KEG) in complex with single-
769 stranded DNA. Amino acids responsible for RNA recognition are labeled in spherical
770 forms. Zn symbolizes the catalytic core.

771 **e,** Schematic illustration of APOBEC3A with its functional domains.

772 **f,** Schematic showing interaction between target EGFP mRNA and CU-REWIRE4.0
773 and 4.X with modified APOBEC3A variants.

774 **g,** Base editing efficiency of EGFP mRNA by CU-REWIRE4.X. The PUF binding site
775 in EGFP is underlined in blue, with adjacent cytosines marked in red (top). Heatmap
776 displays editing rates of cytosines near the on-target site C_{459} for each CU-REWIRE
777 and control (ePUF10 alone), with C_{459} editing rate detailed on the right. Editing rates
778 were measured by RNA-seq with triplicates (refer to methods).

779 **h,** Global editing rates of transcriptome-wide RNA base editing in samples treated with
780 different CU-REWIRE4.X (related to data from panel **g**, labels and cutoff as in
781 Supplementary Fig. 1**e**). Orange rhombuses indicate the on-target site EGFP-C_{459}, and
782 the mean number of off-target editing events is noted beside the dot plots. n represents
783 the total number of edited cytosines detected.

784 **i,** Correlation between on-target editing rates (Y-axis) and transcriptome-wide C-to-U
785 off-target editing events (X-axis) for various CU-REWIRE4s.

Figure 2

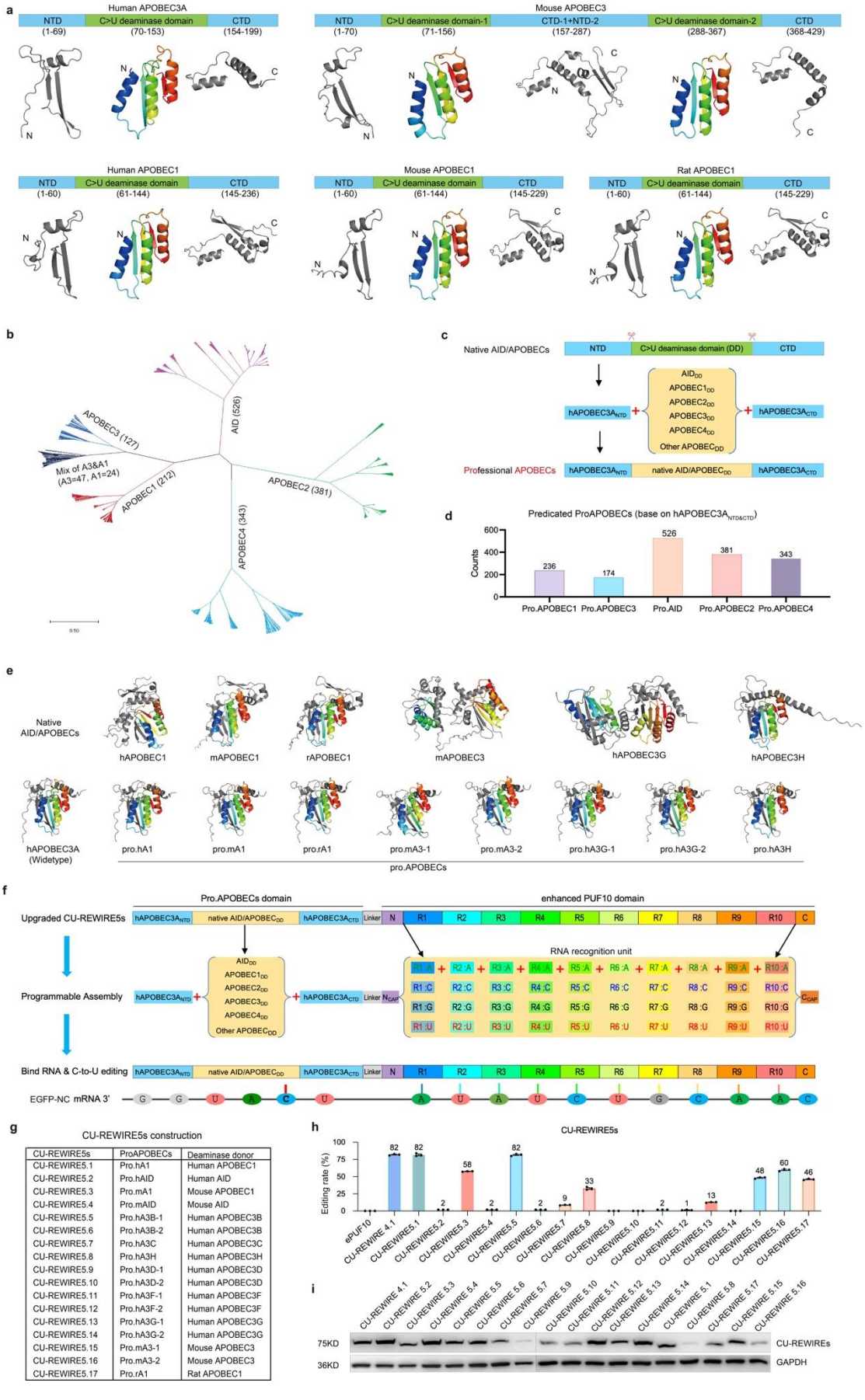

CU-REWIRE5s	ProAPOBECs	Deaminase donor
CU-REWIRE5.1	Pro.hA1	Human APOBEC1
CU-REWIRE5.2	Pro.hAID	Human AID
CU-REWIRE5.3	Pro.mA1	Mouse APOBEC1
CU-REWIRE5.4	Pro.mAID	Mouse AID
CU-REWIRE5.5	Pro.hA3B-1	Human APOBEC3B
CU-REWIRE5.6	Pro.hA3B-2	Human APOBEC3B
CU-REWIRE5.7	Pro.hA3C	Human APOBEC3C
CU-REWIRE5.8	Pro.hA3H	Human APOBEC3H
CU-REWIRE5.9	Pro.hA3D-1	Human APOBEC3D
CU-REWIRE5.10	Pro.hA3D-2	Human APOBEC3D
CU-REWIRE5.11	Pro.hA3F-1	Human APOBEC3F
CU-REWIRE5.12	Pro.hA3F-2	Human APOBEC3F
CU-REWIRE5.13	Pro.hA3G-1	Human APOBEC3G
CU-REWIRE5.14	Pro.hA3G-2	Human APOBEC3G
CU-REWIRE5.15	Pro.mA3-1	Mouse APOBEC3
CU-REWIRE5.16	Pro.mA3-2	Mouse APOBEC3
CU-REWIRE5.17	Pro.rA1	Rat APOBEC1

Fig. 2 | AI-Assisted design of programmable APOBEC platform for engineering ProAPOBEC enzymes.

a, Crystal structure of Human APOBEC3A (PDB: 4XXO), AlphaFold2-predicted structures of native APOBEC proteins: Mouse APOBEC3, Human APOBEC1, Mouse APOBEC1, and Rat APOBEC1, showcasing the NTD, C-to-U deaminase domain, and CTD.

b, Phylogenetic tree of the AID/APOBEC family, with major clades highlighted in different colors.

c, Schematic representation of the assembly of ProAPOBECs.

d, Estimated number of potential ProAPOBEC candidates based on AI-predicted AID/APOBEC deaminase domains.

e, AlphaFold2-predicted structures of AID/APOBEC proteins. Top: AI-predicted structures of native AID/APOBECs. Bottom: AI-predicted structures of ProAPOBECs.

f, The programmable CU-REWIRE5 system with ProAPOBEC variants. Top: Upgraded CU-REWIRE5, featuring integration of ProAPOBEC variants for targeted C-to-U editing. Middle: Schematic depiction of the modular assembly process of CU-REWIRE5. The ProAPOBECs domain, constructed from a selection of natural APOBEC deaminase domains ($APOBEC_{DD}$) derived from various sources, is engineered for specific C-to-U base editing. Accompanying this, the ePUF10 domain includes 10 RNA recognition units, each designed for the specific detection of a unique RNA base type. Bottom: Illustration of the precise engagement of CU-REWIRE5 with the target RNA, showcasing the accurately binding and editing C_{459} of EGFP mRNA.

g, Illustrations depicting the components of CU-REWIRE5, ProAPOBECs, and their deaminase donors.

h, Various editing rates on C_{459} of EGFP mRNA of CU-REWIRE5s, assembled with ProAPOBECs in panel (**i**) and Supplementary Fig. 2**d**.

i, Protein expression levels of CU-REWIRE5s in HEK293T cells. The CU-REWIREs were Flag-tagged, anti-Flag antibody was used to examine CU-REWIREs and GAPDH was used as a loading control.

Figure 3

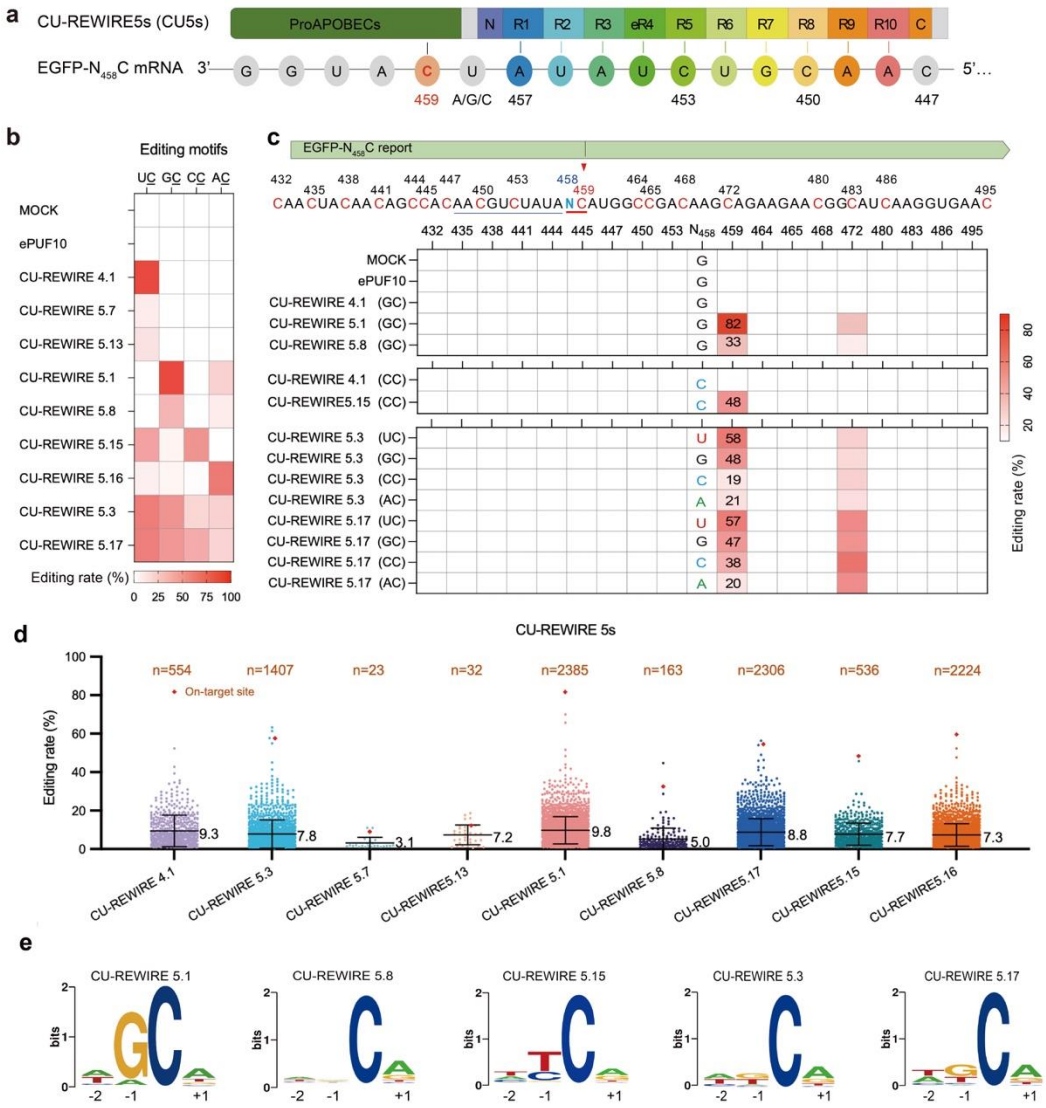

Fig.3 | Enhanced targeting range and specificity in RNA base editing with CU5s.

a, Schematic illustration demonstrating the targeting of the C_{459} site in EGFP mRNA by CU5s. The native $U_{458}C$ context was manually altered to $A_{458}C$, $G_{458}C$, and $C_{458}C$ to test editing preferences.

b, Heatmap depicting the percent editing levels of CU5s at the C_{459} site of EGFP transcript in AC, UC, GC, and CC contexts. The PUF10 binding sequence and on-target site were showed by panel (**a**).

c, Editing efficacy of CU5s at the on-target and bystander site of EGFP transcript in AC, UC, GC, and CC contexts. A heatmap displays editing rates of all cytosines near the on-target site C_{459} for each CU5s and control. Editing rates of C_{459} are measured by RNA-seq with triplicates.

d, Global editing rates of transcriptome-wide RNA-seq by CU5s (related to data from panel **b**, with labels and cutoffs the same as in Fig. 1**g**). Orange rhombuses indicate the on-target EGFP sites, and the average efficiency of total off-target editing events is noted on the right. n numbers represent edited cytosines detected.

e, Sequence motif logos derived from cytosines edited by different CU5s, based on RNA-seq data (related to panel **d**).

Figure 4

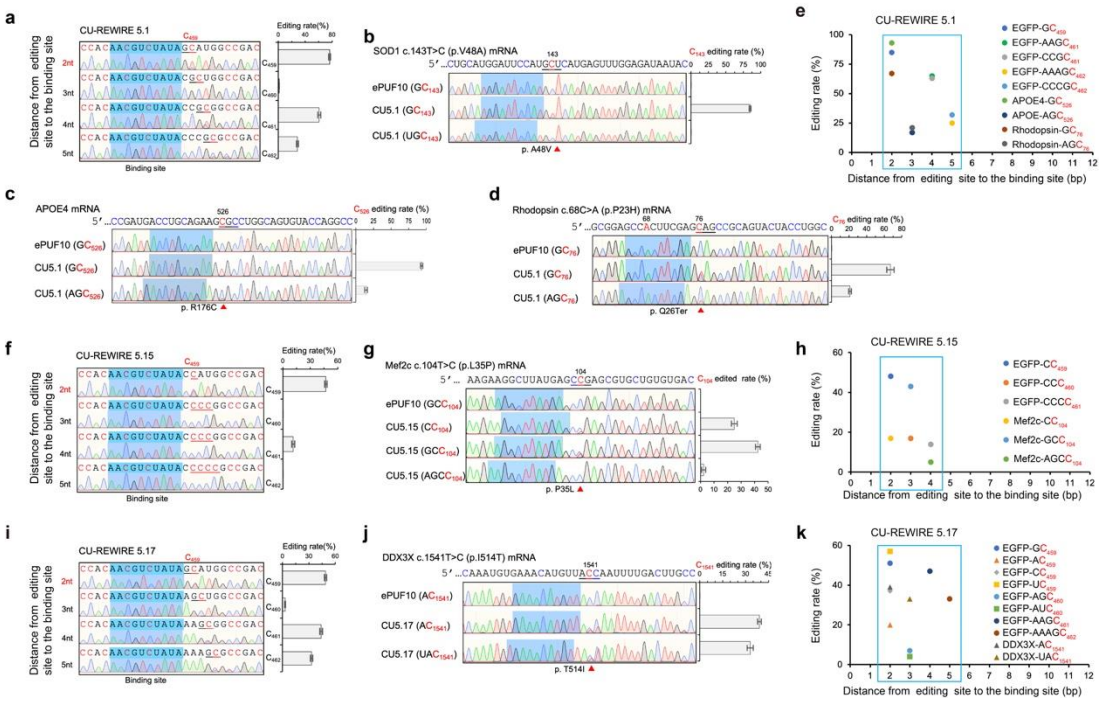

Fig. 4 | Editing windows and application of CU5s.

a, Determination of editing windows for CU5.1 on C_{459} of EGFP mRNA. The graph shows on-target editing rates by CU5.1 at various distances from the PUF binding site. **b-d,** Editing efficacy of CU5.1 on C_{143} of SOD1 reporter mRNA (**b**), C_{526} of APOE4

mRNA (**c**) and C_{76} of Rhodopsin reporter mRNA (**d**) expressed in HEK293T cells. The PUF-binding sites are marked in blue.

e, Summary of the editing window for CU5.1 across EGFP, APOE4, and Rhodopsin reporter mRNAs. The x-axis represents the distance from the editing site to the PUF binding site; the y-axis shows the C-to-U editing rate. Editing rates were acquired by Sanger sequencing.

f, Determination of editing windows for CU5.15 on C_{459} of EGFP mRNA.

g, Editing efficacy of CU5.15 on C_{104} of Mef2c reporter mRNA expressed in HEK293T cells.

h, Summary of the cytosine editing window mediated by CU5.15 around the target sites of EGFP and Mef2c reporter mRNAs.

i, Determination of editing windows for CU5.17 on C_{459} of EGFP mRNA.

j, Editing efficacy of CU5.17 on C_{1541} of DDX3X reporter mRNA expressed in HEK293T cells.

k, Summary of the cytosine editing window mediated by CU5.17 around the target sites of EGFP and DDX3X reporter mRNAs. Values represent mean ± SEM (n=3).

Figure 5

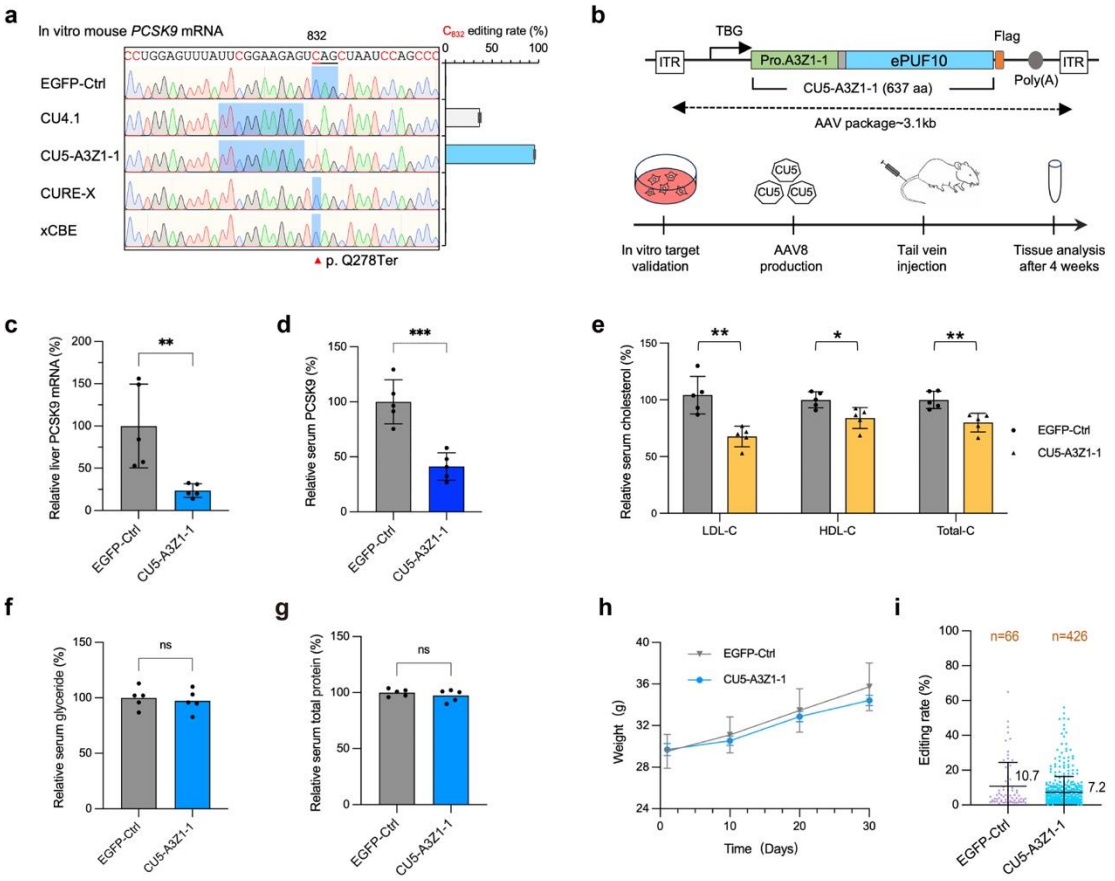

Fig. 5 | *In Vivo* RNA Editing of PCSK9 in Mice reduces cholesterol levels

a, Efficient editing of C_{832} in PCSK9 mRNA by CU-REWIREs and Cas13-based editor. The PUF binding site in PCSK9 is underlined in blue, with on-target site marked in red. Editing rates of C_{832} are measured by Sanger-sequencing with triplicates.

b, Schematic illustration of CU5-A3Z1-1 vectors delivered into mice through intravenous injection of AAV8 virus (top) and the key experimental steps (bottom).

c, In vivo knockdown frequencies induced by CU5-A3Z1-1. Unpaired two-sided Student's t-test was used, statistical values represent the mean ± s.e.m. *P < 0.05. n = 5 mice.

d-g, The levels of serum PCSK9 protein, cholesterol, glyceride and total protein levels in the mice injected with CU5-A3Z1-1. Unpaired two-sided Student's t-test was used, statistical values represent the mean ± s.e.m. *P < 0.05. n = 5 mice.

h, Statistical analysis of weight changes in mice following administration in the CU5-A3Z1-1 and EGFP control. n = 5 mice.

870 **i,** Scatter plots showing transcriptome-wide C-to-U RNA base editing in liver samples
871 treated with CU5-AEZ1-1 and EGFP control in mice. Values represent mean ± s.e.m.
872 (n = 3).

Figure 6

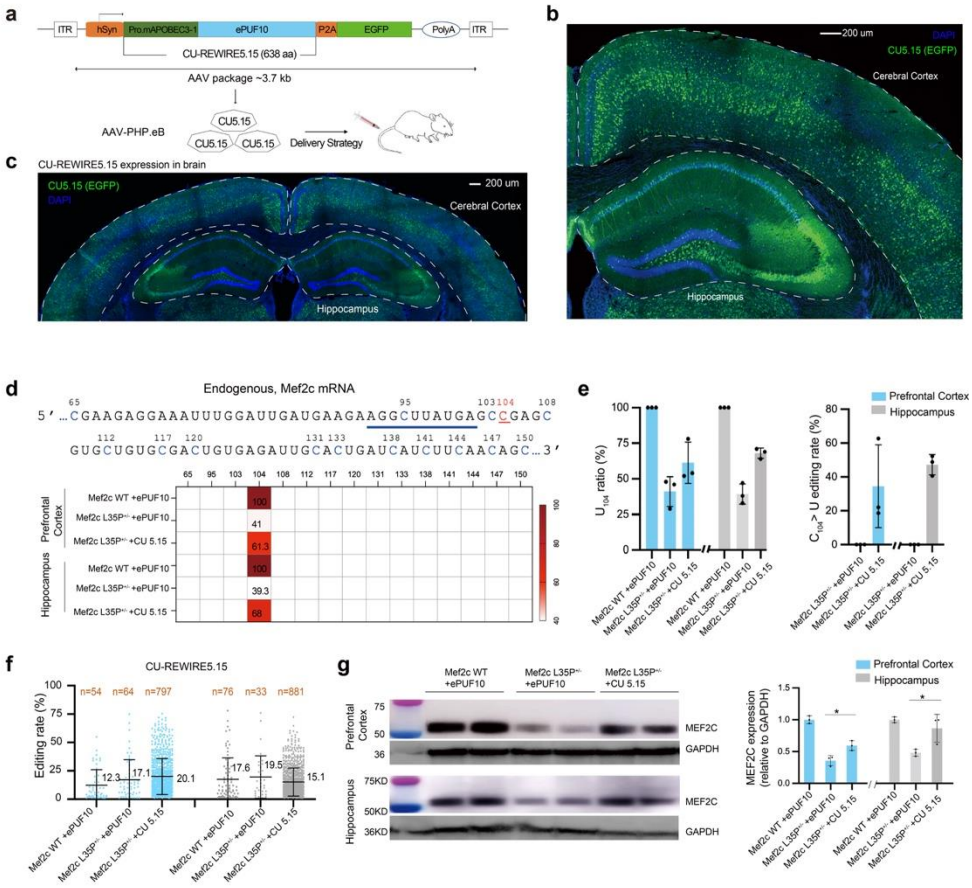

873

874 **Fig. 6 | *In vivo* RNA base editing in Mef2c L35P$^{+/-}$ mice corrects genetic mutations**
875 **and protein expression.**

876 **a,** Schematic illustration of AAV-CU-REWIRE5.15 (CU5.15) vectors delivered into
877 Mef2c L35P$^{+/-}$ mice through intravenous injection of AAV-PHP.eB virus in the tail vein.
878 **b,** Immunofluorescence images showing CU5.15 (green) and DAPI (blue) in the
879 cortical and hippocampal brain regions, 4-weeks post-viral injection. Scale bar: 200μm.
880 **c,** Immunofluorescence images of CU5.15 (green) and DAPI (blue) in the cortical and
881 hippocampal regions, 16-weeks post-viral injection.
882 **d,** Editing efficiency of C_{104} in endogenous mouse Mef2c mRNA by CU5.15. The
883 ePUF10 binding site is underlined in blue, C_{104} marked in red (top). Lower panel:
884 Editing rates of cytosines around the on-target site. Rates were measured by RNA-seq

885 with triplicates. Values represent mean ± s.e.m. (n = 3).

886 **e,** Percentage of U_{104} in prefrontal cortex and hippocampus tissues of Mef2c WT or
887 L35P$^{+/-}$ mice edited by ePUF10 or CU5.15, measured by RNA-seq with triplicates
888 (Left). Editing efficiency of C-to-U of the Mef2c C_{104} site by CU5.15 in various groups
889 (Right). Editing rate formula: $C_{edited} = (U_{CU5.15} - U_{ePUF10}) / C_{total} (1 - U_{ePUF10})$.

890 **f,** Scatter plots showing transcriptome-wide C-to-U RNA base editing in prefrontal
891 cortex or hippocampus samples treated with CU5.15 and ePUF10 control in mice brain
892 samples. Values represent mean ± s.e.m. (n = 3).

893 **g,** MEF2C protein levels in the prefrontal cortex or hippocampus of Mef2c WT or
894 L35P$^{+/-}$ mice treated with ePUF10 or CU5.15. anti-MEF2C antibody was used.
895 GAPDH used as a loading control (Left). Quantification of MEF2C protein level
896 (Right). ePUF10 vs. CU5.15 in prefrontal cortex, P = 0.0203; ePUF10 vs. CU5.15 in
897 hippocampus, P = 0.0423), Unpaired two-sided Student's t-test was used, statistical
898 values represent the mean ± s.e.m. *P < 0.05. n = 3 mice.

Figure 7

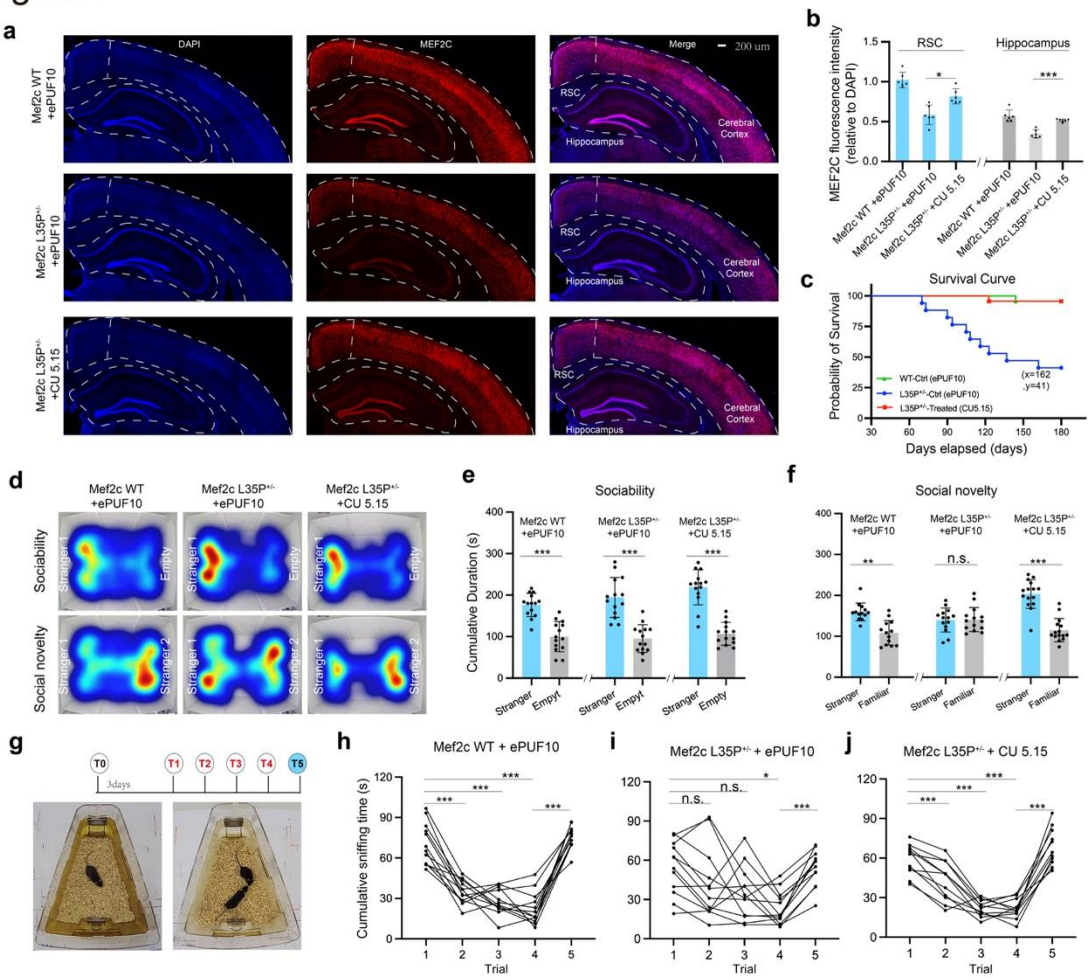

Fig. 7 | *In vivo* RNA base editing in Mef2c L35P$^{+/-}$ mice rescued abnormal social behaviors.

a, Immunohistochemical staining for MEF2C (red) and DAPI (blue) in the retro splenial cortex (RSC) and hippocampus of Mef2c WT and L35P$^{+/-}$ mice, indicating viral injections.

b, Left: Quantification of MEF2C protein fluorescence density in the RSC (ePUF10 vs. CU5.15, P = 0.0040). Right: In the hippocampus (ePUF10 vs. CU5.15, P < 0.0001. *P < 0.01. n = 6 brain slices from three mice of each group).

c, Lifespan of Mef2c L35P$^{+/-}$ mice with ePUF10 or CU5.15. Kaplan-Meier curve statistical analysis (L35P$^{+/-}$(ePUF10) versus L35P$^{+/-}$(CU5.15), Chi square=25.99, P < 0.0001). Kaplan-Meier curve statistical analysis, Log-rank (Mantel-Cox) test was used. WT (ePUF10) n = 23 mice, L35P$^{+/-}$ (ePUF10) n = 17 mice, L35P$^{+/-}$ (CU5.15) n = 23

912 mice).

913 **d,** Heatmaps representing locomotion of Mef2c WT or L35P$^{+/-}$ mice in the sociability
914 and social novelty sessions of the three-chamber test.

915 **e,** Cumulative interaction duration with mouse and empty cage in different groups of
916 Mef2c mice (stranger vs. empty, WT+ePUF10, $P < 0.0001$, L35P$^{+/-}$+ePUF10, $P <$
917 0.0001; L35P$^{+/-}$+ CU5.15, $P < 0.0001$. n = 14 mice).

918 **f,** Cumulative interaction duration with stranger and familiar mouse in different groups
919 of Mef2c mice (stranger vs. familiar, WT+ePUF10, $P = 0.0007$; L35P$^{+/-}$+ePUF10, $P =$
920 0.9130; L35P$^{+/-}$+ CU5.15, $P < 0.0001$. Significantly different, $P < 0.01$. n = 14 mice).

921 **g,** Diagram of the home cage experiment. T0: social isolation for three days. T1-T4:
922 Social interaction trials with one same partner mouse. T5: Social interaction with a
923 novel partner mouse. Recording sniffing time within a 2-minute period.

924 **h,** Sniffing time in social intruder test for Mef2c WT +ePUF10 (T1 vs. T2, $P < 0.0001$;
925 T1 vs. T3, $P < 0.0001$; T1 vs. T4, $P < 0.0001$; T4 vs. T5, $P < 0.0001$. n = 12 mice).

926 **i,** Sniffing time in the social intruder test for Mef2c L35P$^{+/-}$ +ePUF10 (T1 vs. T2, $P =$
927 0.0153; T1 vs. T3, $P = 0.0614$; T1 vs. T4, $P = 0.0026$; T4 vs. T5, $P < 0.0001$. n = 12
928 mice).

929 **j,** Sniffing time in the social intruder test for Mef2c L35P$^{+/-}$ +CU5.15 (T1 vs. T2, $P <$
930 0.0001; T1 vs. T3, $P < 0.0001$; T1 vs. T4, $P < 0.0001$; T4 vs. T5, $P < 0.0001$. n = 12
931 mice).

932 Paired two-sided Student's t-test was used, statistical values represent the mean ± s.e.m.
933 * $P < 0.01$, ** $P < 0.001$, *** $P < 0.0001$.

Figure 1

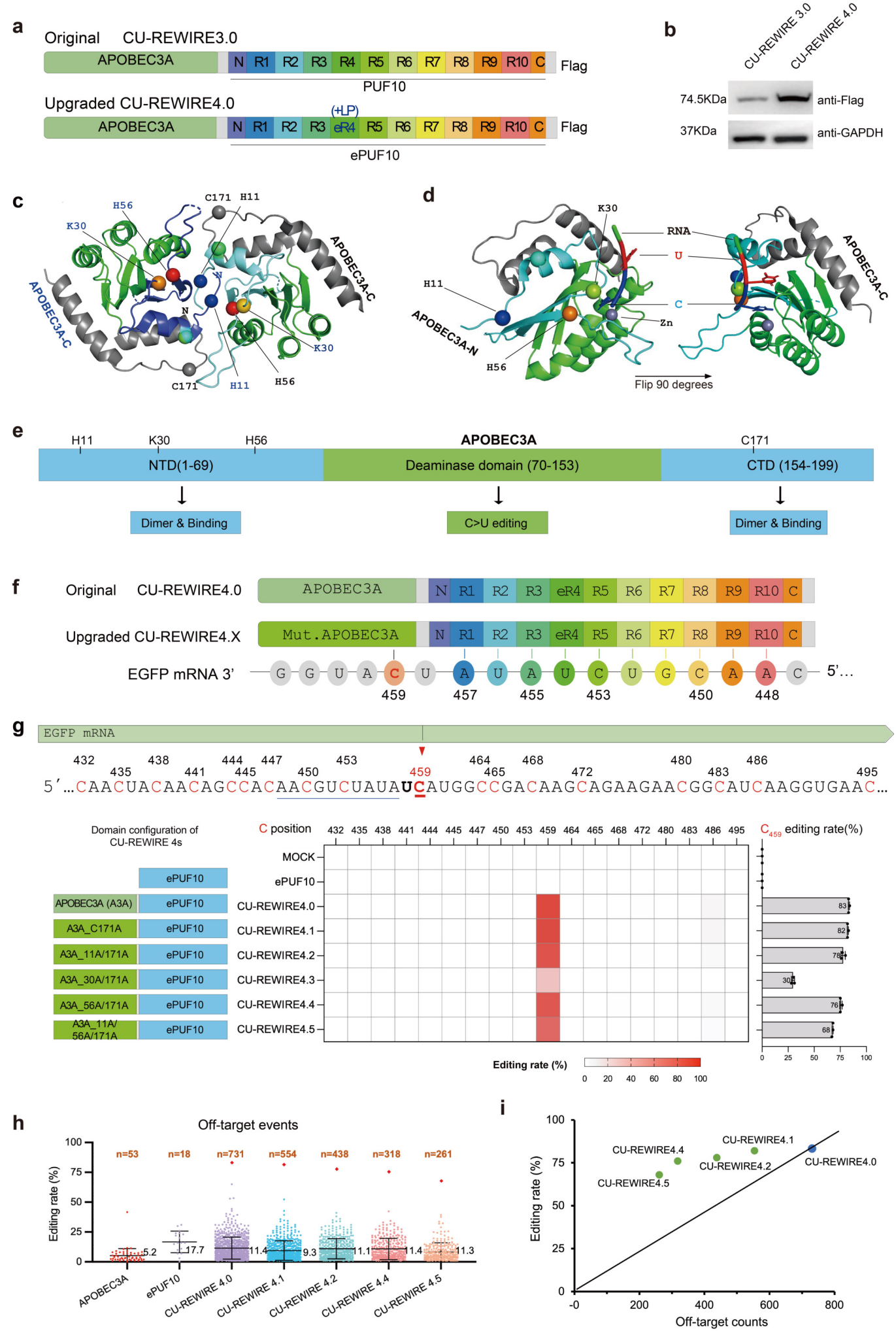
a
Original CU-REWIRE3.0
APOBEC3A
N R1 R2 R3 R4 R5 R6 R7 R8 R9 R10 C
Flag
PUF10
Upgraded CU-REWIRE4.0
(+LP)
eR4
ePUF10
b
CU-REWIRE 3.0
CU-REWIRE 4.0
74.5KDa
anti-Flag
37KDa
anti-GAPDH
c
H56
C171 H11
K30
APOBEC3A-C
APOBEC3A-C
N
K30
C171
H11
H56
d
K30
RNA
U
C
Zn
H11
APOBEC3A-N
H56
APOBEC3A-C
Flip 90 degrees
e
H11
K30
H56
APOBEC3A
C171
NTD(1-69)
Deaminase domain (70-153)
CTD (154-199)
Dimer & Binding
C>U editing
Dimer & Binding
f
Original CU-REWIRE4.0
APOBEC3A
N R1 R2 R3 eR4 R5 R6 R7 R8 R9 R10 C
Upgraded CU-REWIRE4.X
Mut.APOBEC3A
N R1 R2 R3 eR4 R5 R6 R7 R8 R9 R10 C
EGFP mRNA 3'
G G U A C U A U A U C U G C A A C
5'...
459 457 455 453 450 448
g
EGFP mRNA
432 435 438 441 444 445 447 450 453 459 464 465 468 472 480 483 486 495
5'...CAACUACAACAGCCACAACGUCUAUAUCAUGGCCGACAAGCAGAAGAACGGCAUCAAGGUGAAC...
Domain configuration of CU-REWIRE 4s
C position
MOCK
ePUF10
APOBEC3A (A3A)
A3A_C171A
A3A_11A/171A
A3A_30A/171A
A3A_56A/171A
A3A_11A/56A/171A
CU-REWIRE4.0
CU-REWIRE4.1
CU-REWIRE4.2
CU-REWIRE4.3
CU-REWIRE4.4
CU-REWIRE4.5
C459 editing rate(%)
83
82
78
30
76
68
Editing rate (%)
0 20 40 60 80 100
h
Off-target events
Editing rate (%)
n=53 n=18 n=731 n=554 n=438 n=318 n=261
5.2 17.7 11.4 9.3 11.1 11.4 11.3
APOBEC3A
ePUF10
CU-REWIRE 4.0
CU-REWIRE 4.1
CU-REWIRE 4.2
CU-REWIRE 4.4
CU-REWIRE 4.5
i
Editing rate (%)
CU-REWIRE4.1
CU-REWIRE4.4
CU-REWIRE4.2
CU-REWIRE4.0
CU-REWIRE4.5
Off-target counts

Figure 2

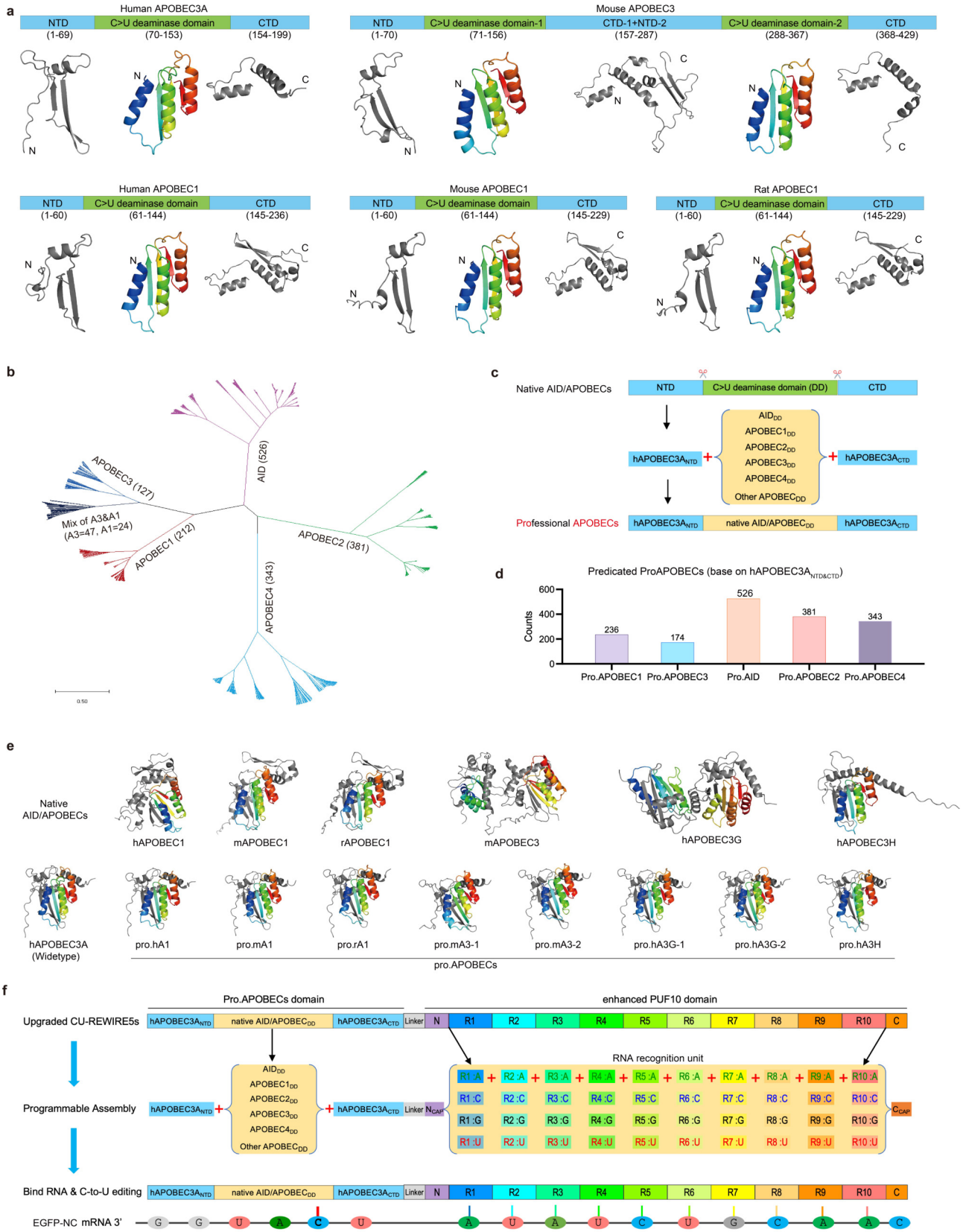

CU-REWIRE5s	ProAPOBECs	Deaminase donor
CU-REWIRE5.1	Pro.hA1	Human APOBEC1
CU-REWIRE5.2	Pro.hAID	Human AID
CU-REWIRE5.3	Pro.mA1	Mouse APOBEC1
CU-REWIRE5.4	Pro.mAID	Mouse AID
CU-REWIRE5.5	Pro.hA3B-1	Human APOBEC3B
CU-REWIRE5.6	Pro.hA3B-2	Human APOBEC3B
CU-REWIRE5.7	Pro.hA3C	Human APOBEC3C
CU-REWIRE5.8	Pro.hA3H	Human APOBEC3H
CU-REWIRE5.9	Pro.hA3D-1	Human APOBEC3D
CU-REWIRE5.10	Pro.hA3D-2	Human APOBEC3D
CU-REWIRE5.11	Pro.hA3F-1	Human APOBEC3F
CU-REWIRE5.12	Pro.hA3F-2	Human APOBEC3F
CU-REWIRE5.13	Pro.hA3G-1	Human APOBEC3G
CU-REWIRE5.14	Pro.hA3G-2	Human APOBEC3G
CU-REWIRE5.15	Pro.mA3-1	Mouse APOBEC3
CU-REWIRE5.16	Pro.mA3-2	Mouse APOBEC3
CU-REWIRE5.17	Pro.rA1	Rat APOBEC1

Figure 3

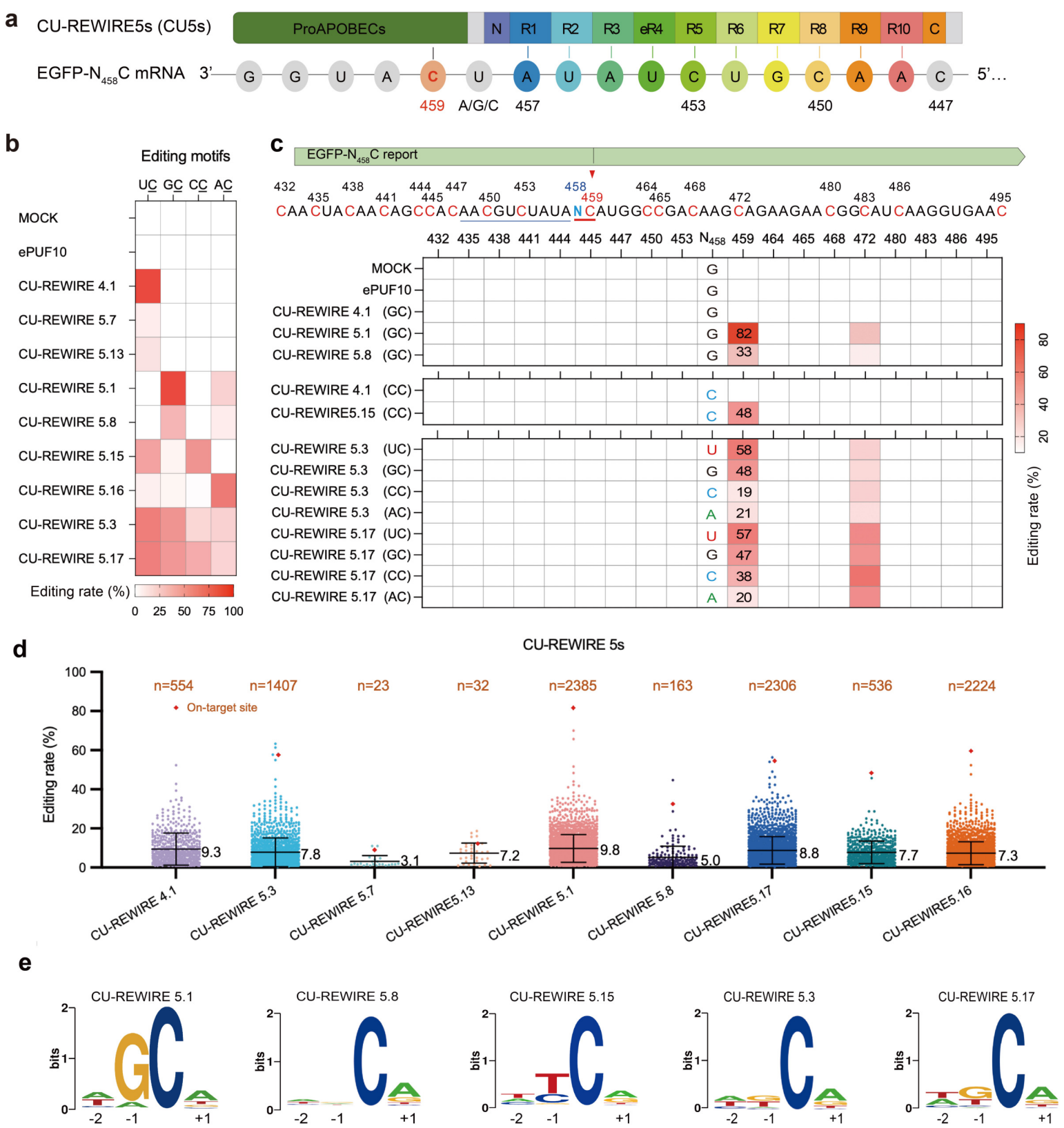
a
CU-REWIRE5s (CU5s)
ProAPOBECs
N R1 R2 R3 eR4 R5 R6 R7 R8 R9 R10 C
EGFP-N458C mRNA 3' G G U A C U A U A U C U G C A A C 5'…
459 A/G/C 457 453 450 447
b
Editing motifs
UC GC CC AC
MOCK
ePUF10
CU-REWIRE 4.1
CU-REWIRE 5.7
CU-REWIRE 5.13
CU-REWIRE 5.1
CU-REWIRE 5.8
CU-REWIRE 5.15
CU-REWIRE 5.16
CU-REWIRE 5.3
CU-REWIRE 5.17
Editing rate (%)
0 25 50 75 100
c
EGFP-N458C report
432 435 438 441 444 447 450 453 458 459 464 465 468 472 480 483 486 495
CAACUACAACAGCCACAACGUCUAUANCAUGGCCGACAAGCAGAAGAACGGCAUCAAGGUGAAC
MOCK
ePUF10
CU-REWIRE 4.1 (GC)
CU-REWIRE 5.1 (GC) 82
CU-REWIRE 5.8 (GC) 33
CU-REWIRE 4.1 (CC)
CU-REWIRE5.15 (CC) 48
CU-REWIRE 5.3 (UC) 58
CU-REWIRE 5.3 (GC) 48
CU-REWIRE 5.3 (CC) 19
CU-REWIRE 5.3 (AC) 21
CU-REWIRE 5.17 (UC) 57
CU-REWIRE 5.17 (GC) 47
CU-REWIRE 5.17 (CC) 38
CU-REWIRE 5.17 (AC) 20
Editing rate (%)
d
CU-REWIRE 5s
Editing rate (%)
n=554 n=1407 n=23 n=32 n=2385 n=163 n=2306 n=536 n=2224
On-target site
9.3 7.8 3.1 7.2 9.8 5.0 8.8 7.7 7.3
CU-REWIRE 4.1
CU-REWIRE 5.3
CU-REWIRE 5.7
CU-REWIRE5.13
CU-REWIRE 5.1
CU-REWIRE 5.8
CU-REWIRE5.17
CU-REWIRE5.15
CU-REWIRE5.16
e
CU-REWIRE 5.1
CU-REWIRE 5.8
CU-REWIRE 5.15
CU-REWIRE 5.3
CU-REWIRE 5.17
bits
-2 -1 +1

Figure 4

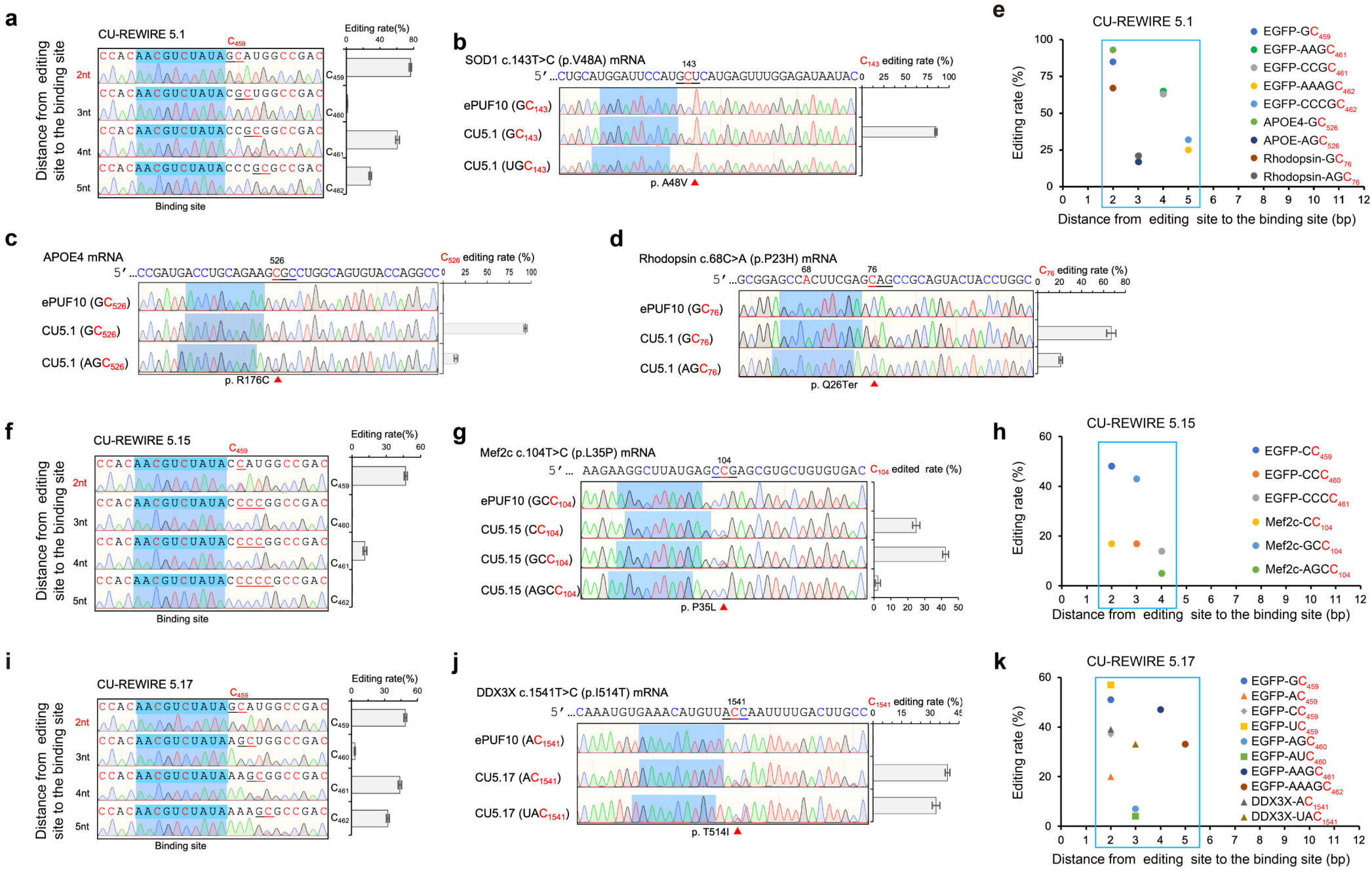
a
CU-REWIRE 5.1
Editing rate(%)
Distance from editing site to the binding site
2nt
3nt
4nt
5nt
Binding site
b
SOD1 c.143T>C (p.V48A) mRNA
ePUF10 (GC143)
CU5.1 (GC143)
CU5.1 (UGC143)
p. A48V
c
APOE4 mRNA
ePUF10 (GC526)
CU5.1 (GC526)
CU5.1 (AGC526)
p. R176C
d
Rhodopsin c.68C>A (p.P23H) mRNA
ePUF10 (GC76)
CU5.1 (GC76)
CU5.1 (AGC76)
p. Q26Ter
e
CU-REWIRE 5.1
Editing rate (%)
Distance from editing site to the binding site (bp)
EGFP-GC459
EGFP-AAGC461
EGFP-CCGC461
EGFP-AAAGC462
EGFP-CCCGC462
APOE4-GC526
APOE-AGC526
Rhodopsin-GC76
Rhodopsin-AGC76
f
CU-REWIRE 5.15
g
Mef2c c.104T>C (p.L35P) mRNA
ePUF10 (GCC104)
CU5.15 (CC104)
CU5.15 (GCC104)
CU5.15 (AGCC104)
p. P35L
h
CU-REWIRE 5.15
EGFP-CC459
EGFP-CCC460
EGFP-CCCC461
Mef2c-CC104
Mef2c-GCC104
Mef2c-AGCC104
i
CU-REWIRE 5.17
j
DDX3X c.1541T>C (p.I514T) mRNA
ePUF10 (AC1541)
CU5.17 (AC1541)
CU5.17 (UAC1541)
p. T514I
k
CU-REWIRE 5.17
EGFP-GC459
EGFP-AC459
EGFP-CC459
EGFP-UC459
EGFP-AGC460
EGFP-AUC460
EGFP-AAGC461
EGFP-AAAGC462
DDX3X-AC1541
DDX3X-UAC1541

Figure 5

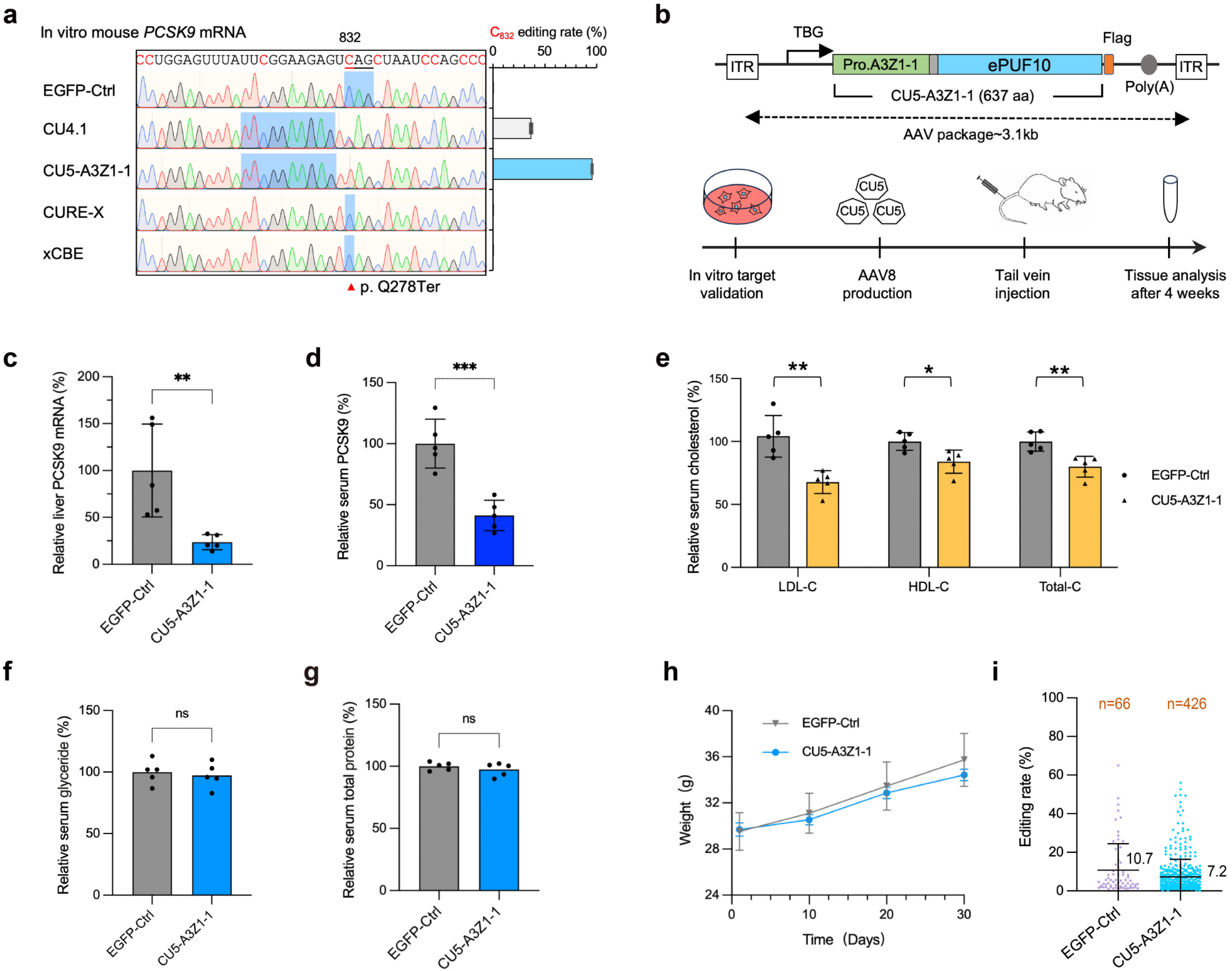
a
In vitro mouse PCSK9 mRNA
832
C832 editing rate (%)
0
50
100
CCUGGAGUUUAUUCGGAAGAGUCAGCUAAUCCAGCCC
EGFP-Ctrl
CU4.1
CU5-A3Z1-1
CURE-X
xCBE
p. Q278Ter
b
TBG
Flag
ITR
Pro.A3Z1-1
ePUF10
ITR
Poly(A)
CU5-A3Z1-1 (637 aa)
AAV package~3.1kb
CU5
CU5
CU5
In vitro target validation
AAV8 production
Tail vein injection
Tissue analysis after 4 weeks
c
Relative liver PCSK9 mRNA (%)
**
EGFP-Ctrl
CU5-A3Z1-1
d
Relative serum PCSK9 (%)
***
EGFP-Ctrl
CU5-A3Z1-1
e
Relative serum cholesterol (%)
**
*
**
LDL-C
HDL-C
Total-C
EGFP-Ctrl
CU5-A3Z1-1
f
Relative serum glyceride (%)
ns
EGFP-Ctrl
CU5-A3Z1-1
g
Relative serum total protein (%)
ns
EGFP-Ctrl
CU5-A3Z1-1
h
Weight (g)
EGFP-Ctrl
CU5-A3Z1-1
Time (Days)
i
Editing rate (%)
n=66
n=426
10.7
7.2
EGFP-Ctrl
CU5-A3Z1-1

Figure 6

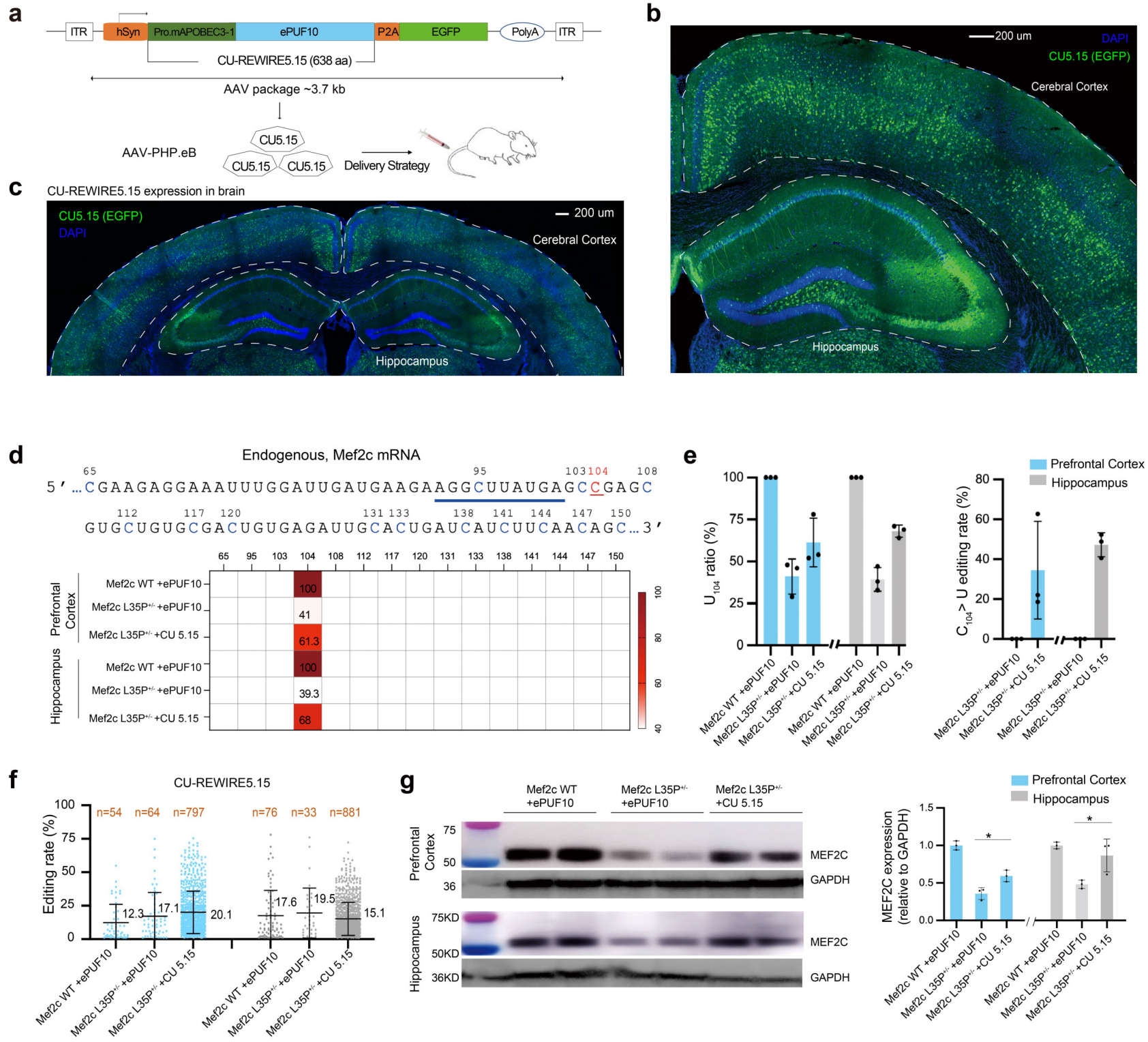
a
ITR
hSyn
Pro.mAPOBEC3-1
ePUF10
P2A
EGFP
PolyA
ITR
CU-REWIRE5.15 (638 aa)
AAV package ~3.7 kb
AAV-PHP.eB
CU5.15
CU5.15
CU5.15
Delivery Strategy
b
200 um
DAPI
CU5.15 (EGFP)
Cerebral Cortex
Hippocampus
c
CU-REWIRE5.15 expression in brain
CU5.15 (EGFP)
DAPI
200 um
Cerebral Cortex
Hippocampus
d
Endogenous, Mef2c mRNA
5′ ...CGAAGAGGAAAUUUGGAUUGAUGAAGAAGGCUUAUGAGCCGAGC
GUGCUGUGCGACUGUGAGAUUGCACUGAUCAUCUUCAACAGC...3′
Prefrontal Cortex
Hippocampus
Mef2c WT +ePUF10
Mef2c L35P+/- +ePUF10
Mef2c L35P+/- +CU 5.15
100
41
61.3
100
39.3
68
e
Prefrontal Cortex
Hippocampus
U104 ratio (%)
C104 > U editing rate (%)
Mef2c WT +ePUF10
Mef2c L35P+/- +ePUF10
Mef2c L35P+/- +CU 5.15
f
CU-REWIRE5.15
Editing rate (%)
n=54
n=64
n=797
n=76
n=33
n=881
12.3
17.1
20.1
17.6
19.5
15.1
Mef2c WT +ePUF10
Mef2c L35P+/- +ePUF10
Mef2c L35P+/- +CU 5.15
g
Mef2c WT +ePUF10
Mef2c L35P+/- +ePUF10
Mef2c L35P+/- +CU 5.15
Prefrontal Cortex
Hippocampus
MEF2C
GAPDH
75KD
50KD
36KD
Prefrontal Cortex
Hippocampus
MEF2C expression (relative to GAPDH)
Mef2c WT +ePUF10
Mef2c L35P+/- +ePUF10
Mef2c L35P+/- +CU 5.15

Figure 7

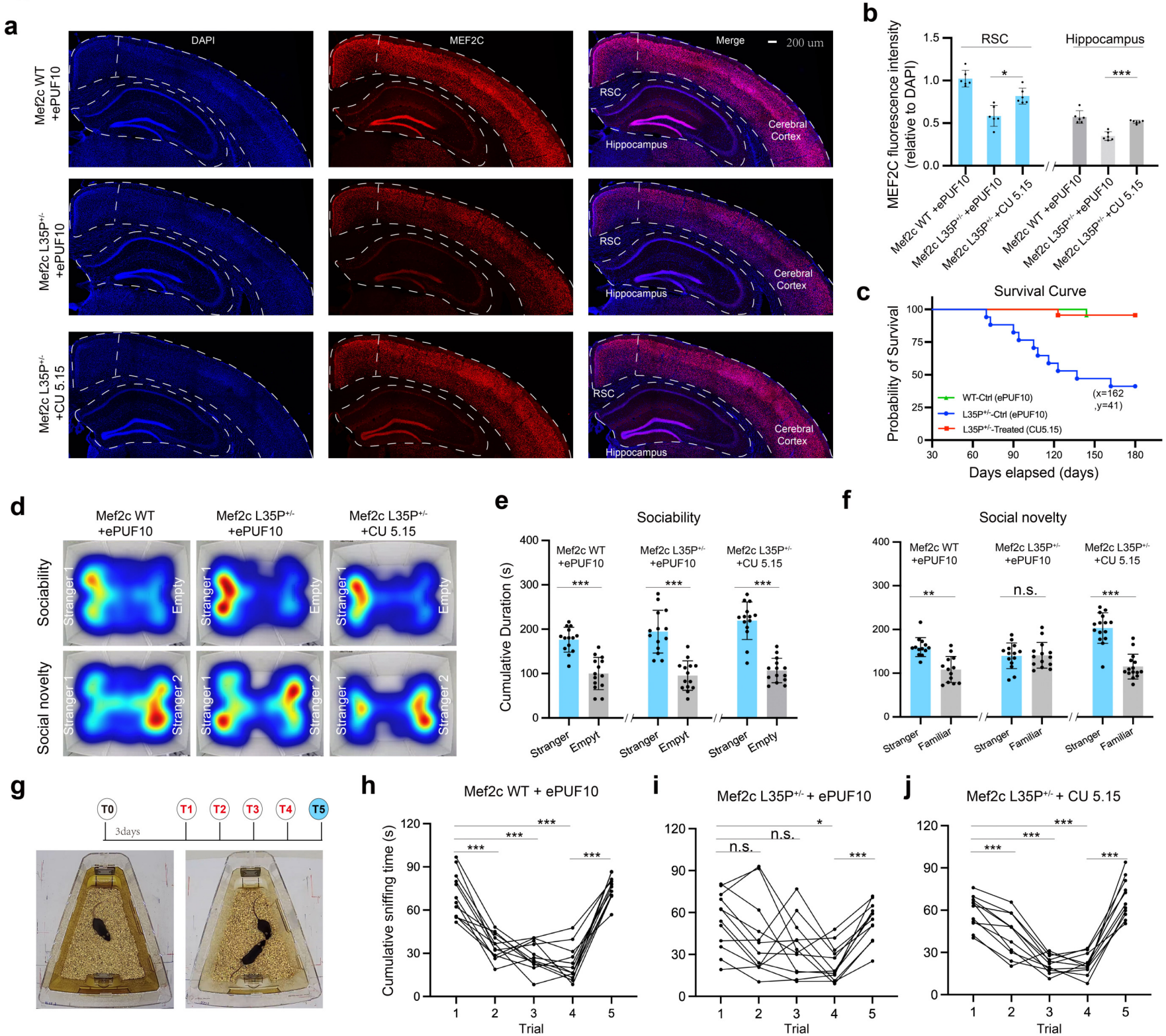
a
DAPI
MEF2C
Merge
200 um
Mef2c WT +ePUF10
Mef2c L35P+/- +ePUF10
Mef2c L35P+/- +CU 5.15
RSC
Hippocampus
Cerebral Cortex
b
MEF2C fluorescence intensity (relative to DAPI)
RSC
Hippocampus
Mef2c WT +ePUF10
Mef2c L35P+/- +ePUF10
Mef2c L35P+/- +CU 5.15
c
Survival Curve
Probability of Survival
Days elapsed (days)
WT-Ctrl (ePUF10)
L35P+/-Ctrl (ePUF10)
L35P+/-Treated (CU5.15)
(x=162 ,y=41)
d
Sociability
Social novelty
Stranger 1
Stranger 2
Empty
e
Sociability
Cumulative Duration (s)
Stranger
Empty
f
Social novelty
Stranger
Familiar
n.s.
g
T0
T1
T2
T3
T4
T5
3days
h
Mef2c WT + ePUF10
Cumulative sniffing time (s)
Trial
i
Mef2c L35P+/- + ePUF10
j
Mef2c L35P+/- + CU 5.15